Salty Matters

John Warren - Wednesday February 28, 2018

Salt Dissolution (5 of 5): Metals and saltflow-focused fluids

Introduction

Most subsurface evaporites ultimately dissolve and, through their ongoing dissolution and alteration, can create conditions suitable for metal enrichment and entrapment in subsurface settings ranging from the burial diagenetic through to the metamorphic and igneous realms. This article looks at a few examples tied to halokinesis, a more comprehensive set of examples and more detailed discussion is given in Chapters 15 and 16 in Warren (2016). Because most, if not all, of any precursor salt mass that helped form these metalliferous deposits via dissolution, has gone, the resulting metal and other accumulations tend to be at or near the edges of salt basins, or in areas where most or all of the actual salts are long gone (typically via complete subsurface dissolution or metamorphic transformation, so that only breccias, weld and indicator mineral suites remain).

A lack of a direct co-occurrence with evaporite salts is perhaps why the metal-evaporite association is not recognised by some in the economic geology community. The significance of disappearing salt masses in focusing and enhancing metal precipitation, via the creation of chloride-rich and sulphate-rich brines, may not be evident without the conceptual tools needed to recognise the former presence of evaporites, post-salt halokinetic structural geometries, and meta-evaporite mineral associations.

The various ore tonnage-grade plots in Warren (2016), shows that many metal accumulations with an evaporite association tend to plot at the larger end of their respective deposit groupings.

Evaporite dissolution helps create "prepared ground."

I am not saying all large metal accumulations require evaporites or the highly-saline subsurface fluids that they can generate. Although, some recent papers do argue for a widespread role of evaporites in a Pb-Zn association (Fusswinkel et al., 2013; Wilkinson et al., 2009) and in sedimentary redbed copper deposits (Rose, 1976; Hitzman et al., 2010).

Typically, the conceptualisation of an evaporite in the economic geology literature is as a bedded evaporite and brine source (Figure 1). Likewise, this article and the relevant chapters in Warren (2016) detail a number of

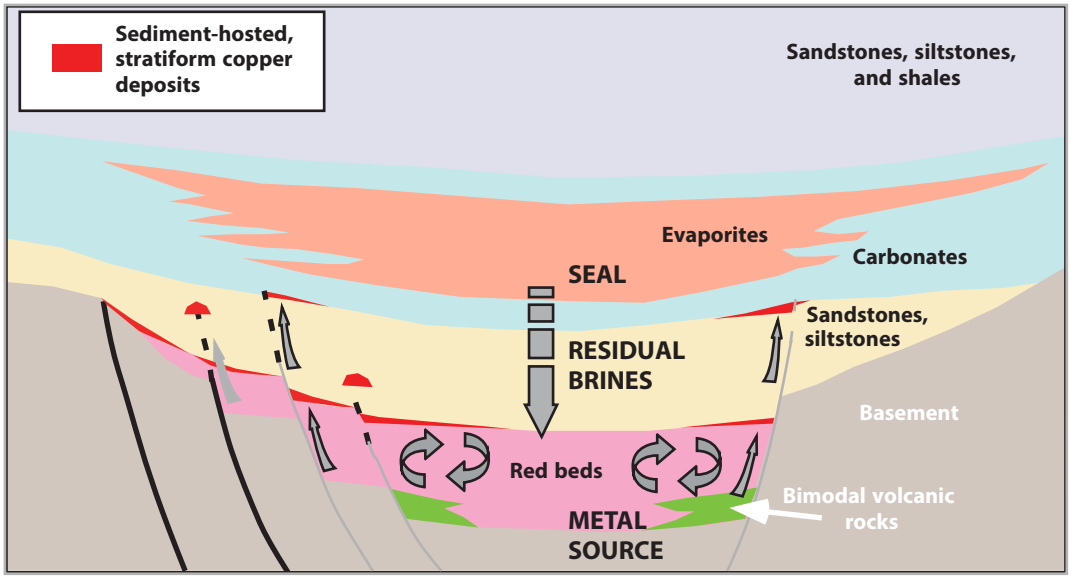

Figure 1. Schematic cross section across an intracratonic, hydrologically closed basin that is typical of those hosting giant and supergiant sediment-hosted stratiform copper deposits (after Hitzman et al., 2010). Syn-rift red beds and minor bimodal volcanic rocks floor the basin. Marine sandstones, siltstones, and shales, which may locally be organic rich, transgressively overlie this red-bed sequence. This siliciclastic sequence grades upward into marine carbonates that contain a thick evaporite sequence. In most productive basins, the evaporites contain significant halite and may have evolved to magnesium and potassium salts. The upper portion of the basin contains shallow marine to continental siliciclastic sediments. The total thickness of the sedimentary sequence may range from several to more than 10 km. The sediment-hosted stratiform copper system consists of residual brines or brines from evaporite dissolution that move downward into the basal, oxidized red-bed sequence. Heat from burial and, in some cases, high heat flow and/or igneous activity initiate convection of these highly saline brines, which are capable of leaching metals from both the red-bed sediments and the basement. Oxidized, metal-rich brines circulate upward to the top of the red-bed sequence, where they encounter organic-rich sediments that provide the reductants necessary to precipitate copper sulphides. Fluids may also utilize fault architecture within the basin to escape to higher levels and precipitate sulphides when they encounter significant zones of either in situ or mobile (natural gas, petroleum) reductants. The evaporite beds provide an effective top seal to the hydrologic system, whereas the basin edges themselves provide lateral containment.

Deposit, Location (Age of Host)		Reserve (10^6 tonnes)	Cu (%)	Pb (%)	Zn (%)	Evaporite Role (relative position and mechanism)	Evaporite Association
DEPOSITS ASSOCIATED WITH BEDDED EVAPORITES OR THEIR RESIDUES							
Redstone River, Canada (Neoproterozoic)	Stratiform -sediment hosted copper (redbed) deposit	small	2.7	-	-	Intersalt stratabound with subsalt focus to upwelling brine	Redbeds with bedded algal limestone host and abundant nodular $CaSO_4$
Creta, Oklahoma, USA (Permian)		1.9	2	-	-	Intersalt bedded (breccia), adjacent redox precipitates	Redbed - evaporitic mudflat host with abundant nodular $CaSO_4$
Corocoro, Bolivia (Eocene)		≥7	≈5	-	-	Intersalt bedded (breccia), brine reductant	Redbed - greenbed host with gypsum and baryte in veinlets and disseminated nodules -nearby diapir. Halokinetic fault focus to basinal fluid escape
Nanisivik, Baffin Island (Mesoproterozoic)	Mississippi Valley Type deposit	6.5	-	1.5	12	Intersalt?, bedded	Host is a stratiform karst cavern: evaporites and pseudomorphs in lateral equivalent beds
San Vincente, Peru (Triassic - Jurassic)		12	-	1	12	Intersalt, bedded. Local supplier of sulphur via TSR	Ore hosted in cryptalgal laminites with pseudomorphs after $CaSO_4$ in barrier-lagoon host
Cadjebut, NW Australia (Devonian)		3.8	-	17% (Pb+Zn)		Intersalt, bedded (breccia). Local supplier of sulphur via TSR	Bedded anhydrite as lateral equivalent to each ore lense and linked by evaporite dissolution breccias. Halokinetic fault focus to basinal metalliferous fluid escape.
Largentiére, France (Triassic)		9.6	-	0.7	3.7	Intersalt	Disseminated $CaSO_4$ cements and nodules within evaporitic lagoonal beds
PERIDIAPIRIC DEPOSITS ASSOCIATED WITH HALOKINETIC EVAPORITE MASSES OR THEIR RESIDUES							
Atlantis II Deep, Red Sea (Holocene)	Stratiform redbed -related copper deposit	150-200	0.8	yes	5-6	Suprasalt allochthon acts as focus to resurging Cu-Zn-Cl brine (salt partially covers ridge basalts)	Dissolving salt allochthon underbelly supplies Cl-rich metalliferous brine to deep seafloor brine lake. Hydrothermal anhydrite is interbedded with laminites
Kupferschiefer-style, Lubin, Poland (Permian)		≈2,000	>2	-	-	Subsalt, stratiform with brine focus creating the Rote Faule contact and adjacent redox precipitates	Anhydrite and halite in Zechstein hangingwall and anhydrite in Rotliegende footwall - redbed ore source
Kupferschiefer-style, Mansfeld, Germany (Permian)		≈7.5	≈2.9	-	±1.8	Subsalt, stratiform with brine focus	Anhydrite and halite in Zechstein hangingwall and anhydrite in Rotliegende footwall - redbed ore source
Dzhezkazgan, Kazakhstan (Carboniferous)		≈400	1.5	0.1-1.0	-	Suprasalt diapiric, anticlinal focus to brine flow	Interbedded redbed and greybed host with $CaSO_4$ and halite in underlying salt anticline and lateral equivalents
Dongchuan deposits, China (Mesoproterozoic)		10-100	1.0-1.5	-	-	Suprasalt allochthon or intrasalt breccia. Allochthon acts as focus to resurging metalliferous brine	Stratabound ore in cryptalgal laminites adjacent to diapiric breccia
Lisbon Valley, Utah, USA (Cretaceous)		small >0.15	1.4	-	-	Suprasalt allochthon, salt movement creates ore-hosting faults in overburden	Ore in vein and pore fills adjacent to faults created by halokinesis
Jubilee, Nova Scotia (Carboniferous)	Mississippi Valley Type Deposit	Not economic	n/a	n/a	n/a	Subsalt allochthon (tectonic breccia) stratiform, subsalt focus to brine flow	Interstratified fractured carbonate and anhydrite ore host created by regional salt-induced gravity slide
Gays River, Nova Scotia (Carboniferous)		2.4	-	8.6	6.3	Subsalt with subsalt focus to upwelling brine. Local supplier of sulphur via TSR	Anhydrite both within main ore zone and as cement in disseminated ore
Bou Grine, Tunisia (Cretaceous)		7.3	-	2.4	9.7	Suprasalt, peridiapiric, brine focus via halokinesis	Ore in peridiapiric organic-rich pyritic laminates adjacent to halite allochthons
Gulf Coast USA (Tertiary)		Not economic	n/a	n/a	n/a	Suprasalt allochthon capstone, brine focus via halokinesis	Anhydritic caprock undergoing bacteriogenic alteration in association with reservoired hydrocarbons

Table 1. Classic ore deposit breakdown (stratiform redbed-related Cu versus MVT Pb-Zn deposits) of some of the many Phanerzoic-Neoproterozoic base-metal deposits formed in the diagenetic realm in association with bedded, dissolving and flowing evaporites (see Warren 2016 for more detail on these and additional salt dissolution-related deposits).

megagiant ore deposits where dissolving evaporite bodies have contributed in some way to a metal accumulation (Table 1). However this current article, like Warren 2016) focuses on the mechanisms and indicators tied to a halokinetic-ore association. Halokinesis is an aspect of evaporites that is not widely discussed in the field of ore deposit models.

High levels of metals that typify ore deposits, like thick salts in evaporite basins, are responses to unusual conditions, bot associations are related to fortuitous interactions of local and plate-scale tectonics with basin-scale fluid systems. To become an ore deposit, amounts of metal need to build, at specific precipitation sites, to levels well above that of their background presence in the carrier brines. This typically requires a chemical interface that can be related to salinity/oxidation, or cooling/heating interfaces. As such, it is no surprise that the same process sets created by conductivity and salinity/oxidation levels, and tied to dissolution and reprecipitation of minerals, are likely to be associated with conduits formed by the passage of pore waters across chemical and temperature interfaces created by altered buried evaporites and associate hydrothermal fluids and salts (e.g., Warren 2016; Fusswinkel et al., 2013; Salty Matters blog, April 29, 2016).

Not all sediment-associated ore deposits are associated with evaporites. Only in those ore deposits classified as anorogenic and/or continental margin can subsurface evaporite masses can be involved in the same unusual concentration and alteration conditions that lead to the creation of metalliferous ore deposits (evaporite associations are indicated by E in Figure 2). At other times and locations hydrothermal mineral salts, especially anhydrite ($CaSO_4$)which can supply sulphur as it dissolves, can be an integral part of the ore accumulation, but their occurrence may be unrelated to aridity. Hydrothermal anhydrite and other burial/magmatic hydrothermal salts tend to form in high salinity conditions inherent to the ore-forming environment and not necessarily to the presence of precursor evaporites; as in the formation of carbonatites (e.g. Afrikanda and Bayan Obo; Wu, 2008), or pegmatites and some IOCG deposits (hydrothermal anhydrite is indicated by HA in Figure 2). In some such hot subsurface settings the role of any nearby buried true" evaporite may be, via its dissolution or alteration, to aid in the creation of highly-saline high-temperature basinal brines (Chapter 16; Warren, 2016). According to whether the resulting brines are chloride or sulphate-rich, they can act as either enhanced metal carriers or fixers.

The role of evaporites creating metalliferous ores is two-fold; 1) In solution (halite-dominant precursor) they can act as chloride-rich metal carriers and 2) Locally, as $CaSO_4$ beds or masses alter and disintegrate, their dissolution products, especially if trapped, can supply sulphur (mostly via bacteriogenic or thermogenic H_2S). Dissolutional interfaces set up chemical interfaces that act as foci during brine mixing so manufacturing conditions suitable for precipitation of metal sulphides or native elements. As a consequence, most evaporite-associated ore systems tend to epigenetic, rather than syngenetic. Subsurface salt beds and masses are merely the solid part of a sizeable ionic recycling system, dissolved metals are another part, and zones of mixing between the two are typically sites where metal sulphides tend to gather.

At the world-scale, both evaporite and ore systems are driven by plate tectonics. Halite-dominated sequences, deposited in the drawdown basin centres, tend to dissolve in burial, and so supply chloride ions to the brine system. Salt beds that are thick enough tend to flow and thus focus the

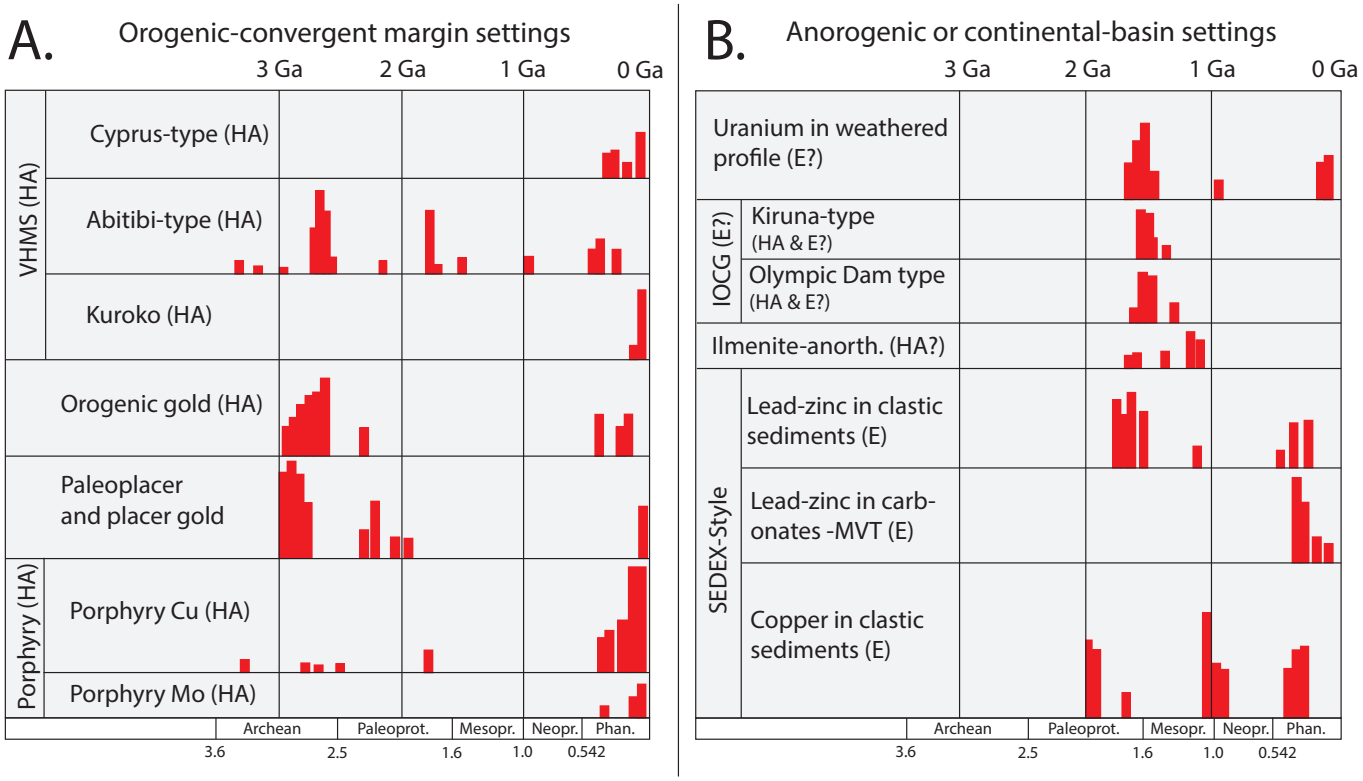

Figure 2. Ore deposit occurrences across geological time (modified from Groves et al., 2005; see Meyer 1988 for more detail and other igneous subsets). E indicates direct evidence of evaporites or derived brine in the formative processes associated with some of the examples of this deposit style. E? indicates the presence of hypersaline brine associated with the formative ore process. Such brines may be magmatic or sedimentary/hydrothermal. HA indicates the presence or former presence of hydrothermal or igneous anhydrite precipitated by non evaporitic processes.

upward and centripetal passage of basinal and hydrothermal fluid flows. Dissolving gypsum or anhydrite beds, typically deposited higher on the basin platform or diagenetically accumulated along salt dissolution edges and salt welds (touchdowns) can supply sulphur, via bacterial or thermochemical sulphate reduction, while simultaneously focusing the subsalt metalliferous brine flows into the precipitation interface.

When the chemistries of the dissolving salt beds and the metal carriers interact so that redox fronts, salinity contrasts, and other precipitative interfaces are set up, an ore deposit can form. Thus, in base and precious metal exploration in evaporitic terranes, we are ultimately searching for those parts of a subsurface ionic cycling system where the salt dissolution, salt beds and metal systems have interacted to create economic levels of metalliferous precipitates.

Modelling

Conceptually, this evaporite-related notion of regional fluid flow in a sedimentary/metasedimentary host is somewhat different to the internal process and local mineralised halo models that dominate our understanding of those world-class ore deposits related to the interior workings of igneous systems. The latter is known as an orthomagmatic system where internal igneous processes of fractional crystallisation and liquid immiscibility largely control ore formation. Ores are deposited in an evolving framework of world-scale tectonics and magmatism across time, from Archaean greenstones to those of present-day sialic plate tectonism. Examples, where buried evaporites have been assimilated into a magma chamber, are discussed chapter 16 in Warren, 2016. Then there are the various ore deposits that are external to (paramagmatic) or unrelated to the emplacement of igneous bodies (nonmagmatic). In both cases, the mineralisation is typically part of an ongoing long-term sedimentary burial history, tied to dissolving and flowing salt masses and associated hydrothermal circulation.

Evidence for hydrothermally-induced low-moderate temperature mineralisation is often best preserved in textures in the hydrothermally altered rock matrix, typically located outside the actual ore deposit (in its hydrothermal alteration halo). From the hydrothermal fluid perspective, one should see the role of evaporites and metal sulphides as each contributing its part to a larger scale "mineral systems" paradigm; much in the same way as, in a petroleum system, the integration of concepts of source, carrier, seal and trap are fundamental requirements to understand and predict economic oil and gas accumulations.

This holistic ore systems approach is not fully encompassed in some economic geology studies that use sequence stratigraphic sedimentological approaches for ore deposit prediction in greenschist terrains (Ruffel et al. 1998; Wilkinson and Dunster, 1996). In my opinion, this approach can shift the interpretation paradigm too far into the depositional realm. The problem with classic sequence stratigraphic criteria, when trying to understand ore genesis, is that sequence stratigraphy does not handle well the concept of a mobile ephemeral subsurface salt body that climbs the stratigraphy via autochthonous and allochthonous process sets (halokinesis). As the salt flows, it dissolves and so brings with it the associated epigenetic influences of brine-driven diagenesis and metasomatism.

Current sequence stratigraphic paradigms in the economic geology realm are dominated by the assumption that the geometry of the units in the depositional system, and associated fault characteristics, are relatively static within the buried sediment prism. Yet, in terms of most sediment-hosted hypersaline ore deposits, what is most important in understanding the metal-evaporite association is the understanding of; 1) Evaporite dissolution and halokinesis, 2) Migration of subsurface fluids, 3) Creation of shallower or lateral-flow redox fronts along with, 4) Opening and closing of fault/shear focused fluid conduits, typically tied to, the coming and going of bedded and halokinetic salts. These factors, rather than primary sediment wedge geometries, are the dominant controls as the mineralising system passes from the diagenetic into the metamorphic realm.

It is interesting that in a benchmark paper, discussing and classifying the world's ore deposits in a plate-tectonic-time framework, Groves et al., (2007) list almost all the major ore categories shown in Figure 2b as belonging to the group of "...sediment-hosted deposits of non-diagnostic or variable geodynamic setting." Into this category, they place all stratiform to stratabound sediment-hosted deposits with variable proportions of Pb, Zn, Cu (including Zambian Copper belt, Kupferschiefer and SedEx deposits). They go on to note (p. 26) that, although there is general agreement that the majority of these various deposits formed during active crustal extension, either in intracratonic rift basins or passive margin sediment hosts, there is considerable controversy concerning their broader scale tectonic setting at the time of mineralisation and the driving force for hydrothermal fluid flow at the time of their mineralisation.

Perhaps this lack of model specificity in the varied interpretations of sediment-hosted deposits reflects the fact that one piece of significant information is missing from many ore genesis models. Namely, that the greater majority of these poorly classified sediment-hosted deposits sat atop, or adjacent to, or beneath, what were once thick evaporite sequences (Table 1). In many cases, the salt mass is long gone. It was the dissolution of these salt masses, either bedded or halokinetic-allochthonous, that focused much of the ore-fluid flow in the sedimentary-diagenetic realm. The loss of salt as the basin sediments passed from the low temperature diagenetic into the metamorphic realm, and as the metalliferous fluid flow was focused into permeable conduits about, below or above the dissolving and retreating, or flowing salt edges, is how salt-related ore deposits form.

This is why the majority of these salt-aided deposits tend to occur outside salt basins that retain substantial salt masses still in the diagenetic realm. The deposits are a response to the dissolution and flow of evaporites, or the residual seawater bitterns created in underlying and subjacent settings as the salt beds were deposited, not to the presence of actual undissolved primary evaporite masses. As we see in Proterozoic and Archaean meta-evaporites and most Precambrian evaporite associations, the original salt mass is long gone from the hosting succession, via varying combinations of halokinesis, dissolution and metasomatism (Warren, 2016, Chapter 13; Salt Matters blog, August 28, 2016).

Ore deposits of Precambrian tend to be linked to evaporite alteration products and residues and rarely preserve actual sedimentary salts (other than local remains of minor hydrothermal anhydrite). In younger Phanerozoic deposits, such as Kupferschiefer, the Atlantis II deep and Dzhezkazgan, portions of actual salt (brine source) can remain in the more deeply buried parts of the basin.

Metal sulphide precipitates are not rare or unique in the subsurface diagenetic fluid milieu, what is essential in the prediction of ore-grade levels of metal sulphide buildups is understanding where and why the metal precipitation system is focused into particular structurally-controlled positions and encompass time frame/fluid volumes sufficient to build an ore deposit.

That is, evaporite-associated ore deposits are no more than ancient subsurface hydrology-specific associations where the precipitation system was stable enough, for long enough, to allow higher, ore-grade levels of metals sulphides to accumulate from carrier brines at particularly favourable and stable chemical and temperature interfaces. As such, metal precipitation sites are part of an ore-forming process set, spread across the epigenetic and syngenetic realms (Table 1). They are part of the regional evolution of the fluid plumbing from the time of deposition, into burial, and on into the realm of metamorphic transformation. This means to understand the ore system tied an evaporite-entraining system holistically; one must integrate local ore paragenesis with various aspects of the basin-scale geology, sedimentology, sequence stratigraphy, diagenetic-metamorphic-igneous facies, fluid flow conduits and structural evolution of the evaporitic basin.

Metals with a halokinetic focus

To illustrate the importance of salt dissolution tied to halokinetic fluid focusing I have chosen two well-known deposits, one is a stratiform redbed copper association (Corocoro deposit), the other a SedEx style Pb-Zn deposit (McArthur River or HYC deposit)

Corocoro and other sandstone-hosted deposits of the Central Andes

Stratabound deposits of copper (±Ag), hosted by variably-dipping continental clastic sedimentary rocks, occur in Central Andean intermontane basins and are known to postdate compressive deformation/uplift events in the region (Flint, 1986, 1989). The deposits are relatively small with variable host-rock depositional ages and include; Negra Huanusha, central Peru (Permo-Triassic); Caleta Coloso, northern Chile (Lower Cretaceous); Corocoro, northwestern Bolivia (Oligo-Miocene); San Bartolo, northern Chile (Oligo-Miocene); and Yasyamayo, northwestern Argentina (Miocene-Pliocene).

The Corocoro area has produced the largest amount of copper in these Andean examples, something like 7.8 million tonnes of copper at a grade of 7.1% (Cox et al., 2007). The location of mineralisation is controlled by structurally-focused redox fronts in bedded sediment hosts, which abut a steeply-dipping translatent thrust fault (Figure 3). Deposits are irregular, usually elongate lenses of native metal, sulphides, and their oxidation products. Typically, deposits are hosted in alluvial fan and playa sandstones or conglomerate facies that also contain abundant gypsum and lesser halite. The undersides of some copper sheets at Corocoro even preserve mudcrack polygons and bed-parallel burrow traces (Savrda et al., 2006). Ore mimicry of mudcracks is not a feature controlled by on-for-one-replacement of organic material deposited in a sandstone; rather it is following pre-existing permeability/redox contrasts.

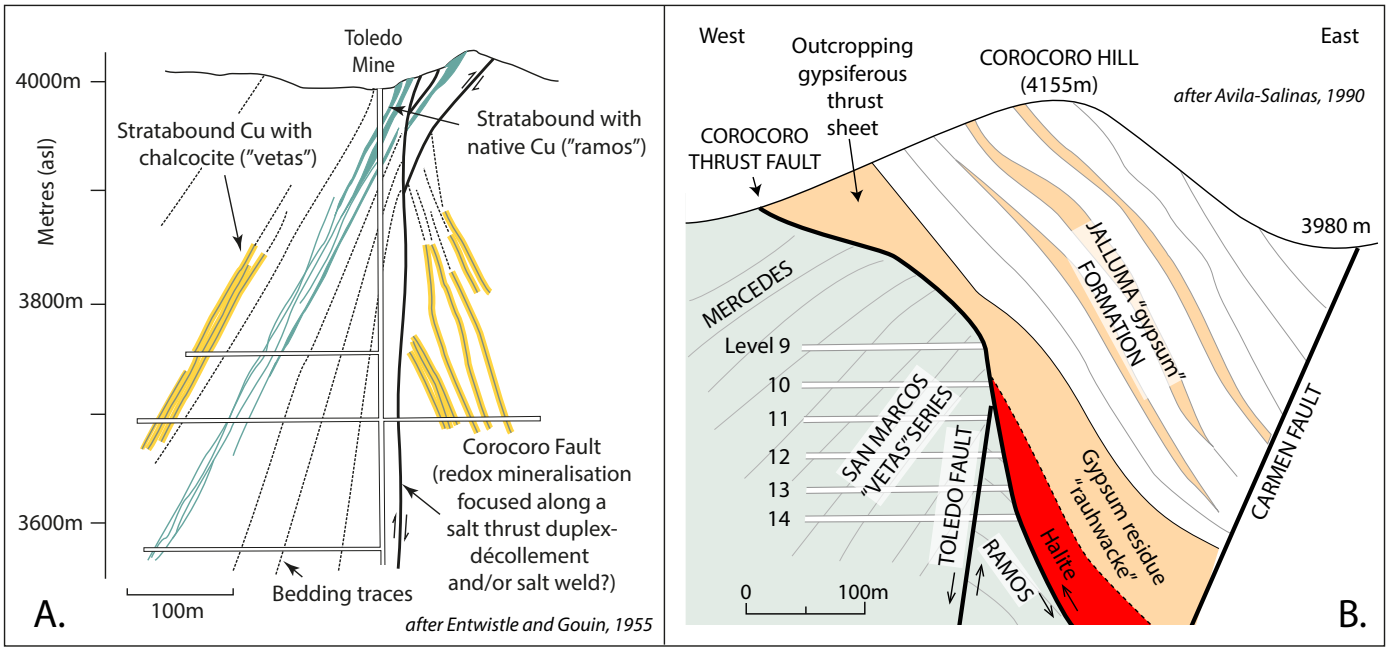

Figure 3. Cross sections of the Toledo mine in the Corocoro ore district. A) Adapted from Entwistle and Gouin (1955).he influence of the Corocoro fault as a ore control was recognised and similarieies with the African copper belt noted, but the evaporite was not considered to be the major ore control B) Adapted from Avila-Salinas (1990). The evaporite-cored thrust fault was recognised as a salt décollement and mapped as a halokinetic feature, but ore was considered to be sediment-hosted and the brine focus related to the dissolving and focusing control of the salt thrust was not emphasised.

Corocoro deposits have been mined sporadically since they were first exploited by the local Indians, prior to the Spanish invasion in the 16th century and were largely exhausted in half a century of more intense mining operations that began in 1873 (Figure 3). Sandstone and conglomerate matrices show evidence of bleaching and leaching of the original redbed host with numerous red-greybed redox interfaces visible in the mined sequences. Ore minerals (dominantly native copper) are secondary fills within secondary intergranular pores created by the dissolution of earlier carbonate and sulphate masses and intergranular cement. Twelve grey sandstone beds, which were host to the long worked-out native copper ores, occur within a stratigraphic thickness of 60 m, in a unit known as the Ramos Member that still hosts abundant $CaSO_4$ as gypsum (Figure 3).

Ores are stratabound, but not necessarily stratiform, and the larger masses of native copper are typically shallower and present as vein fills. Sometimes the copper pseudomorphs large orthogonal-ended aragonite prisms, which can be several centimetres across. There are two main styles of mineralization; 1) Ore minerals as a matrix to stratiform detrital silicates, typically low dipping and commonly highlighting primary sedimentary structures, such as cross stratification, 2) Ores in stacked channelized sand bodies, that show steep dips in structurally complex and folded zones with local brecciation (Figure 3). Native copper commonly fills thin laterally extensive sheets in tectonic fractures in the limbs of tight folds. Ljunggren and Meyer (1964) interpreted these folded diagenetic sheets of copper as a remobilization products precipitated during deformation of earlier matrix-pore filling copper.

Critical factors in Corocoro ore genesis include (Flint, 1989; Aliva-Salinas, 1990): 1) Stratigraphic association of evaporites, organic-rich lacustrine mudstones, clastic reservoir rocks, and orogenic, igneous provenance areas for both basin-fill sediments and metals; and 2) Intrabasinal evolution of metal-mobilising saline brines derived from the buried and dissolving lacustrine evaporites that flush volcaniclastics, volcanics and feldspathic sediments. The same saline diagenetic fluids also caused the dissolution of early, framework-supporting cement and large aragonite prisms, all now pseudomorphed by native copper. Avila-Salinas (1990) notes the presence of a salt-cored décollement and its likely tie to some of the highly saline sodium chloride brines found at depth in the vicinity of the Toledo Mine (Figure 3b)

The ore-hosting clastic horizons are consistently located in the highly gypsiferous Vetas Member of the Ramos Formation, which was deposited as redbeds in braidplains or fluviodeltaic playa margins centripetal to the edges of saline evaporitic lakes that were accumulating gypsum and halite (Figure 4; Flint, 1989). Abundant gypsum is still present in the Ramos Member as nodules and satinspar vein fills. Both are secondary evaporite textures likely implying the dissolution of previously more voluminous $CaSO_4$ and NaCl beds and masses. Gypsum along with celestite are the most common gangue minerals associated with native copper veins in all the Corocoro deposits (Singewald and Berry, 1922). In the geological analysis of the first two decades of last century, the copper-bearing beds of the westerly-dipping series were called "vetas" and those of the easterly-dipping beds "ramos" and, as a matter of convenience, the names became attached to the rocks themselves. The term "veta" is Spanish for vein and "ramo" the Spanish for branch (native copper). The 1922 paper by Singewald and Berry noted that the veta horizons were traceable continuously for over 5 km in outcrop, but they found no apparent primary trends related to ramos outcrops (Figure 3).

Six mineralised layers of each kind were in exploited in mining during the first two decades of last century, the thicknesses of which varied from a few centimetres to 7 meters (Figure 3). Sheets and masses of native copper, called charque, were up to 600 pounds in weight, but more significant volumes of copper were extracted from vetas sandstones where copper was found as diffuse minute grains, pellets, or granular masses of the native metal. Associated with the enriched copper zones were more oxidised minerals as malachite, chrysocolla, azurite, domeykite, and chalcocite. Singewald and Berry (1922) noted gypsum and salt were the principal gangue minerals, while silver minerals were rare. The vetas sediment hosts tended to be coarser grained, often conglomeratic; whereas the ramos sediment hosts were finer-grained with copper present as smaller particles and masses.

The currently accepted interpretation of the Corocoro copper is that it formed during early diagenesis within a saline playa depositional environment, and in combination with dissolution of the adjacent bedded lacustrine evaporites (Figure 4). This bedded combination is thought to have controlled the formation, transport and precipitation of the copper ore (Flint, 1989). Playa sandstones, sealed between impervious evaporitic mudstone layers, created the plumbing for focused metalliferous fluid migration toward the basin margin. It is argued that the carbonaceous material at Corocoro was likely concentrated in the sandstones and conglomerates and not in the shalier members of the sedimentary sequence (Eugster, 1989).

The organics were considered strata-entrained as primary plant matter (e.g. spores) preferentially in the sandstones, along with later possible catagenic/hydrothermally cracked products migrating as hydrocarbons out of the basin. This created locally reducing pore environments in the aquifers wherever these reduced fluids met with somewhat more oxidising updip pore waters. This updip migration of saline reducing waters, in combination with sulphur supplied as H_2S from the adjacent dissolving calcium sulphate beds and nodules, as well as from dissolving intergranular sulphate cement, precipitated copper in the newly created secondary porosity. The pore water chemistry and flow hydrology of this sandstone-hosted Cu system is thought to show many affinities with diagenetic uranium-redox precipitating systems, as defined by Shockey and Renfro (1974).

However, there is, in my mind, a possible anomaly in this model, which assumes organics were deposited in fluvial sandstones at the time of deposition. It is highly unusual to have higher plant material accumulating in large volumes in sandstone in a setting that is sufficiently arid and oxidising to precipitate ongoing interbeds of halite and gypsum. Such settings are typically too dry to allow abundant higher plant growth. Also, groundwaters that are flowing basinward through bajada sandstones in Neogene sediments of the Andes are ephemeral or too oxidising to facilitate the long-term reducing conditions needed to preserve significant volumes of high plant remains in the sandstone aquifers.

What is also interesting in this sedimentological/diagenetic model of Tertiary age cupriferous redbeds deposits in the Andes, centred on Corocoro, but not considered in any detail in the published literature base, is the question..., What controlled the folding, and the associated brecciation and perhaps even subsurface brine interfaces responsible for the Cu precipitation? All the stratabound Bolivian Cu deposits accumulated in sediment hosts that were deposited in fault-bound intermontane

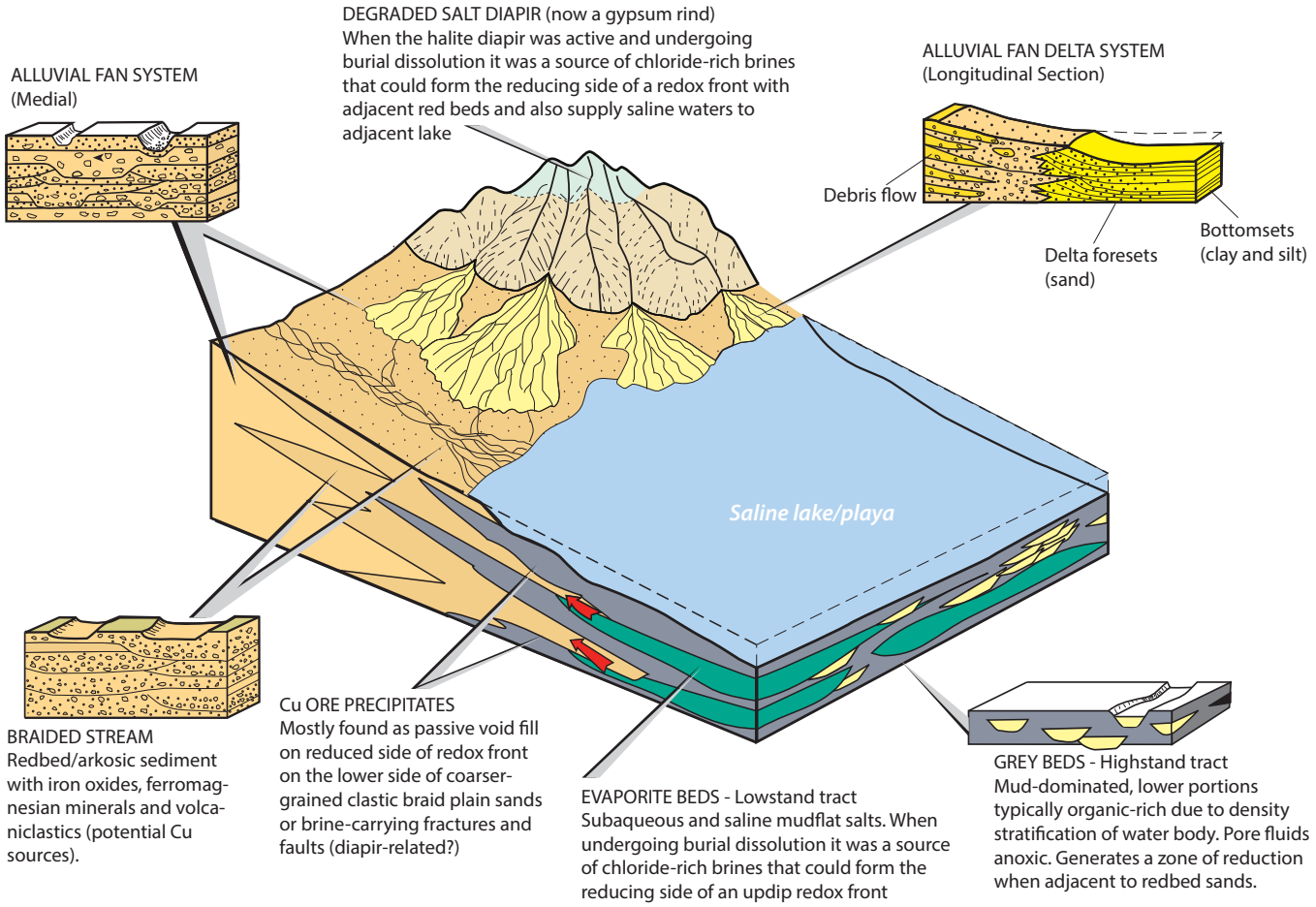

Figure 4. Sedimentological model for precipitation of Corocoro ores showing source of metalliferous chloride brines by early burial dissolution of bedded evaporites or diapir or salt-décollement dissolution (or both) and the resultant setup of the Cu-precipitating redox front (in part after Flint 1989; Warren, 2000).

groundwater sumps. All are located in hydrologic lows in the crustal shortening tectonic scenario that typifies the Tertiary history of the Andes.

The variable ages of the host sediments and the predominance of evaporite indicators including gypsum in outcrop (often as diagenetic residues, not primary, features in the fluvial hosts) and all intimately tied to the Corocoro ore forces the question...., "was the fluid focusing driving the Cu precipitation a response to compression-driven halokinesis in an evolving salt-lubricated thrust belt?" Did this on-ground scenario occur in a halokinetic hydrology, that was possibly related to a combination of thrust-driven telogenesis, redox setup, evaporite dissolution and aquifer focusing of brines with dissolution aiding local slumping? This, along with associated strike-slip prisms, could better explain the stability of redox interfaces in sandstone aquifers across timeframes needed to accumulate significant native copper volumes. After all, most of the ore textures are passive precipitates, mainly in pre-existing porosity. If so, perhaps these deposits are not a variation on a roll-front uranium theme, which is predicated on dispersed primary organic material in the host sandstones (Shockey and Renfro, 1974).

When one plots the position of Corocoro and other redbed copper across the region, the 1000-lb gorilla that has been standing in the corner of the room for the past century becomes obvious. The Corocoro redbed copper deposit is located on a salt-cored fault system linked across less than a kilometre to an outcropping gypsum-capped remnant of a salt diapir which crosscuts the anticlinal axis of a saline redbed/greybed Corocoro sequence and ties to the saline decollement of the Corocoro Fault (Figure 5). The same tie to salt-cored decollement and diapir proximity is true of other nearby redbed copper deposits to the south-southeast, such as Veta Verde and Callapa. It is highly likely that the saline fluid interfaces forming the redbed Cu deposits of Corocoro, Veta Verde and Callapa were halokinetically focused. A similar-salt lubricated set of thrusts and strike-slip faults typifies halokinetic anticline outcrops in Central Iran.

It is highly likely that much of the structuration that is controlling Corocoro ore positioning is a response to salt flow related uplift, brine conduits and fracture creation. Metal precipitation occurred at redox interfaces induced and controlled by regional salt-lubricated compressional tectonism, and the associated salt-structuration has driven the brine-interface redox hydrology.

Work by Rutland (1966) did make an observation that the Corocoro ore deposits are related to an unconformity between the Ramos and Vetas Formations. Previously, the unconformity was interpreted as directly due to the outcrop of the Corocoro Fault. He noted that the fault and the unconformity were one and the same. In the 1960s there was no notion of a salt weld but it was nonetheless a highly astute observation by Roy Rutland. He went on to note a similar unconformity is tied to the growth

Figure 5. Corocoro district, Bolivia. Satellite image showing a gypsum-capped salt diapir that outcrops in a salt thrust décollement around a kilometer north of the main Corocoro deposits. Location is plotted using SaltWork version 1.6 mounted on the public version of the Bing® image base.

of the Chuquichambi salt diapir, some 100 km southeast of Corocoro. Unfortunately, the halokinetic implications of Rutland's work were not considered 20 years later in Flint's key 1989, paper inferring a mostly clastic sedimentological origin for the Corocoro and other similar SSC deposits.

A possible halokinetic/weld association also leads to the question... Were the salt lakes, that are considered an integral part of the depositional and saline ore-precipitation systems at Corocoro by Flint, also a response to dissolution of the same nearby diapiric structures, when they were active in the mid to late Tertiary? This tie, between diapir/weld brines sourced in the drainage hinterland and bedded evaporite - lacustrine mud interbeds accumulating in the groundwater outflow sumps, is the case with groundwater inflow for the Salar de Atacama infill, as it is in other Quaternary salt lakes in the region. The are many diapir remnants across the Andes region. It seems that the Corocoro style of Cu mineralisation is perhaps another example of suprasalt redox focusing in a halokinetic setting.

Whether the halokinetic scenario, or the currently accepted non-halokinetic bedded arid-lacustrine evaporite scenario, explains the Cu mineralisation Corocoro is yet to be tested. But in terms of future copper exploration for similar deposits, it probably requires an answer. A halokinetic association offers an exploration targeting mechanism, utilising satellite imagery and aerial/gravimetric data, prior to the acquisition of on-ground land positions and geochemical surveys.

McArthur River (HYC), Ridge II and Cooley II deposits, Australia

This material on the HYC deposit will be expanded upon in an upcoming paper by Lees and Warren (in prep.). Before mining, the McArthur River (or HYC) Pb-Zn-Ag deposit, contained 227 million tonnes of 9.2% Zn, 4.1% Pb, 0.2% Cu and 41 ppm Ag (Logan et al., 1990; Pirajno, and Bagas, 2008). The deposit is hosted in the HYC Pyritic Shale member and lies adjacent to the Emu Fault in the McArthur Basin and adjacent to what are currently sub-economic base metal deposits in the Emu Fault zone known as the Cooley II and the Ridge II deposits (Figure 6a). Across all these deposits, major ore sulphides are pyrite, sphalerite and galena, with lesser chalcopyrite, arsenopyrite and marcasite. The mineralised region has an area of two km2 and averages 55 m in thickness (Figure 6b). It is elongated parallel to the major Emu growth Fault, which lies 1.5 km to the east, but is separated from the main ore mass by carbonate breccias of the Cooley Dolostone Member (Figure 6a-d).

The sequence at McArthur River comprises dolomites of the Emmerugga Dolostone (with the Mara Dolostone and Mitchell Yard members), overlain by the Teena Dolostone with abundant aragonite splays indicative of a normal-marine tropical Proterozoic carbonate. Overlying the Teena Dolostone in the vicinity of the HYC deposit is the somewhat deeper water Barney Creek Formation and its equivalents, containing the W-Fold Shale member, while the ore is hosted in carbonaceous shales, with multiple lenses of fine-grained galena-sphalerite-pyrite, separated by inter-ore sedimentary breccias (Large et al., 1998). This unit contains numerous sedimentary features indicative of a deeper-water anoxic setting. For example, comparison with $\delta^{13}C$ values from isolated kerogen in the HYC laminites confirms that n-alkanes in Bitumen II are indigenous to HYC, indicating that the deposit formed under euxinic conditions. This supports a generally-held model for Sedex deposits the region, whereby lead and zinc reacted in a stratified water column with sulphide produced by bacterial sulphate reduction (Holman et al., 2014).

The ore-hosting organic-rich 1,643-Ma HYC Pyritic Shale Member of the Barney Creek Formation is much thicker in the HYC sub-basin than elsewhere in the Batten Trough Fault Zone (e.g., Glyde River Basin) and consists mainly of dolomitic carbonaceous siltstones (Figure 7; Davidson and Dashlooty, 1993; Bull 1998). I would argue this thickening reflects a combination of long-term local basinfloor subsidence, related to salt withdrawal, and brine stratification due to ongoing salt dissolution and focused outflow. Indicators of former salt allochthon tiers are widespread in the vicinity of the HYC deposit, but are absent in the Glyde River Basin.

Breccias in and around HYC

In the HYC mine area, the ore interval is overlain by the HYC pyritic shale member and made up of pyritic bituminous and dolomitic shales and polymict breccias (Figure 7). Importantly, when contacts are walked

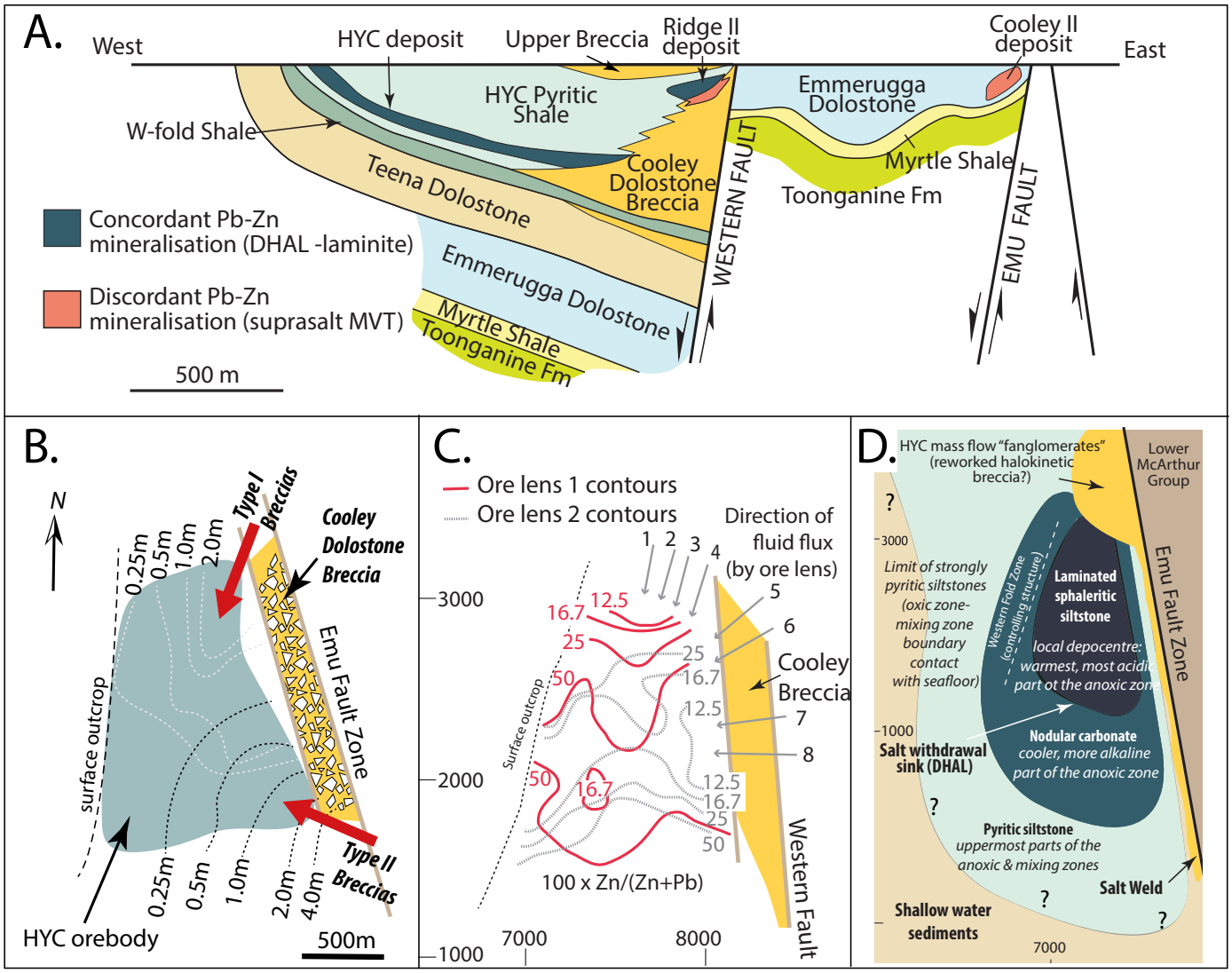

Figure 6. McArthur River (HYC) Pb-Zn deposit. A) Schematic E-W cross-section. B) Isopachs of maximum clast size for Type I and Type II breccias, with arrows showing inferred transport direction. C) Combined plot showing the up-section change in the orientation of metal zonation within the deposit, and the contours of the ratio 100xZn/(Zn+Pb) for the lowermost and uppermost ore lenses. Arrows depict the interpreted direction of fluid flux through the mineralising system during formation of each ore lens D) Schematic plan view showing the likely synsedimentary spatial relationship between pyritic siltstones, nodular carbonates, and base metal-mineralized siltstones in the HYC subbasin. Fault control of the eastern basin margin and impingement of a fanglomerate wedge in the north (adapted from Walker et al., 1977; Logan, 1979: Perkins and Bell, 1998; Ireland et al., 2004a,b).

out in outcrop, the polymict breccias are significantly transgressive to bedding, while drilled intersections in the vicinity of the HYC deposit and in the mine itself show the breccias are stratabound. Another interesting feature of these breccias is that they can contain mineralised clasts. More broadly, a variety of sedimentary breccias occur throughout the Barney Creek Formation stratigraphy, especially along the eastern margin of the HYC half graben and tend to pass updip into the breccias of the Cooley Dolostone (Figure 6a).

Williams 1976, defined three breccia types (I, II and III) in the HYC area. Type I breccia beds occur in the lower half of the HYC Pyritic Shale Member and contain clasts characteristic of lithologies in formations of the McArthur Group below the Barney Creek Formation (Table 2). In the northern end of the sub-basin, the breccias are of a chaotic nature with no sorting and minor grading of clasts (Figure 6b). The underlying shale beds are frequently contorted and squeezed between the breccia fragments, which reach a maximum size of approximately 10 m. Toward the south, the thickness and maximum clast size of individual breccia beds decrease (Figure 6b). All breccia units are thickest adjacent to the Emu Fault Zone and likely record sediment sinks controlled by rapid fault-controlled basin subsidence during Barney Creek time. Inter-ore breccias amalgamate and thicken to the north-north-east of HYC, and occupy a position toward the foot of what is interpreted as a more substantial breccia lens, dominated by sediment gravity flow deposits (Figure 6d; Logan et al., 2001).

In a subsequent study, Ireland et al. (2004a) identified four distinct sedimentary breccia styles within Type I breccias: framework-supported polymictic boulder breccia; matrix-supported pebble breccia; and gravel-rich and sand-rich graded turbidite beds (Table 2). The boulder breccias can be weakly reverse-graded and show rapid lateral transition into the other facies, all of which are interpreted as more distal manifestations of the

Walker et al., 1977		Ireland et al., 2004a		This article
Type I	Occur in the lower half of the HYC Pyritic Shale Member and contain clasts characteristic of lithologies in formations of the McArthur Group below the Barney Creek Formation. In the northern end of the sub-basin, the breccias are of a chaotic nature with no sorting and very little grading of clasts (Figure 18b). The underlying shale beds are frequently contorted and squeezed between the breccia fragments which reach a maximum size of approximately 10 m. Towards the south the thickness and maximum clast size of individual breccia beds decrease. Towards the south, the thickness and maximum clast size of individual breccia beds decrease.	Framework-supported polymictic boulder breccia.	Occasionally weakly reverse graded and typically show rapid lateral transitionsinto the other facies, all of which are interpreted as distal manifestations of the same sedimentary events.	Evaporite dissolution breccia left after the dissolution of a laterally-extensive salt allochthon dissolution carapace that once covered (sealed) an active (now dissolved) salt allochthon tongue, which had flowed across the seafloor. Weak reverse grading passing up into mosaic breccia is indicative of a salt dissolution breccia.
		Matrix-supported pebble breccia.	Reflect mass-flow initiation as clast-rich debris flows, with transformation via the elutriation of fines into the subsequent turbulent flow from which the turbidite and matrix-supported breccia facies were deposited.	Typical mass flow and turbidite features that intertongue with DHAL laminites, as seen in many salt tongue associated deep seafloor sumps in the Gulf of Mexico and the Mediterranean.
		Gravel-rich and sand-rich graded turbidite beds.		
		Sand-rich graded turbidite beds.		
Type II	Occur throughout the HYC Pyritic Shale Member but are most common in the upper half of the Member. Clasts are predominantly grey dololutite which occasionally contain radiating clusters of acicular crystal pseudomorphs ("coxcos"). The clasts are similar to lithologies in the Emmerugga and Teena Dolomites and are considered to have been derived from these formations. A characteristic of this breccia type, which differentiates it from Type I and III breccias is the absence of green and red clasts, signifying that clasts were not derived from the Tooganinie or lower formations. Type II breccias lack the well-developed grading seen in many Type I breccias.	Not considered by Ireland et al., 2004a, b		Evaporite dissolution breccia left after the dissolution of a fault or salt-weld bound structure. Prior to compression, loss of salt and collapse the initial salt feature may have been a diapiric structure and a feeder to a DHAL on the nearby seafloor. Diapir ablation breccias typically contain a range of clasts plucked from adjacent lithologies during the rise of the salt mass.
Type III	Type III breccia beds are confined to the uppermost breccia unit of the HYC Pyritic Shale Member in the HYC sub-basin and are equivalent to the Upper Breccia of Murray (1975). This unit consists exclusively of Type III breccias with the exception of several shale beds near the base. The top of the Upper Breccia is not exposed in the sub-basin, and the unit reaches a maximum known thickness of 210 m. Clasts within the breccias are completely chaotic, and there is no recognisable grading or sorting. Clasts range in size from a few millimetres up to several tens of metres. The fragment lithologies are identical to those in the Type I breccias with the important exception that they also contain clasts of sandstone, quartzite and potash-metasomatized quartz dolerite—lithologies that are characteristic of the Masterton Formation. The fragments are therefore considered to be derived from the McArthur Group (below the Barney Creek Formation) and the Masterton Formation. The most likely source of the clasts from the Masterton Formation was considered to the horsts in the Emu Fault Zone, but the exact source area and the direction of movement of the clasts could not be identified by the authors.			Evaporite dissolution breccia left after the dissolution of a laterally-extensive salt allochthon tongue that once covered (sealed) the underlying DHAL sediment as it flowed across the seafloor. A modern partial analogue (but on land, not deep seafloor) is forming as the debris carapace and salt apron at Kuh-e-Namak (Qom) in Iran (Warren, 2008, 2016 for detail)

Table 2. Origin of salt-related HYC breccias

same sedimentary events. The flow geometry and relationships between these breccia styles are interpreted by Ireland et al. (2004a) to reflect mass-flow initiation as clast-rich debris flows, with transformation via the elutriation of fines into a subsequent turbulent flow from which the turbidite and matrix-supported breccia facies were deposited.

All the Type 1 mass-flow facies contain clasts of the common and minor components of the in-situ laminated base-metal mineralised siltstone. Texturally these clasts are identical to their in-situ counterparts and are distinct from other sulphidic clasts that are of unequivocal replacement origin. In the boulder breccias, intraclasts may be the dominant clast type, and the matrix may contain abundant fine-grained sphalerite and pyrite. Dark-coloured sphaleritic and pyritic breccia matrices are distinct from pale carbonate-siliciclastic matrices, are associated with a high abundance of sulphidic clasts, and systematically occupy the lower parts of breccia units. Consequently, clasts that resemble in-situ ore facies are confirmed as genuine intraclasts incorporated into erosive mass flows before complete consolidation. Disaggregation and assimilation of sulphidic sediment in the flow contributed to the sulphide component of the dark breccia matrices. The presence of laminated sulphidic intraclasts in the mass-flow facies constrains mineralisation at HYC to the uppermost part of the seafloor sediment pile, where this material was susceptible to erosion by incoming clast-rich mass flows. That is, the presence of laminated sulphidic intraclasts in the mass-flow facies constrains mineralisation at HYC to the uppermost part of the seafloor sediment pile, where this material was susceptible to erosion by incoming clast-rich mass flows (Ireland et al., 2004a).

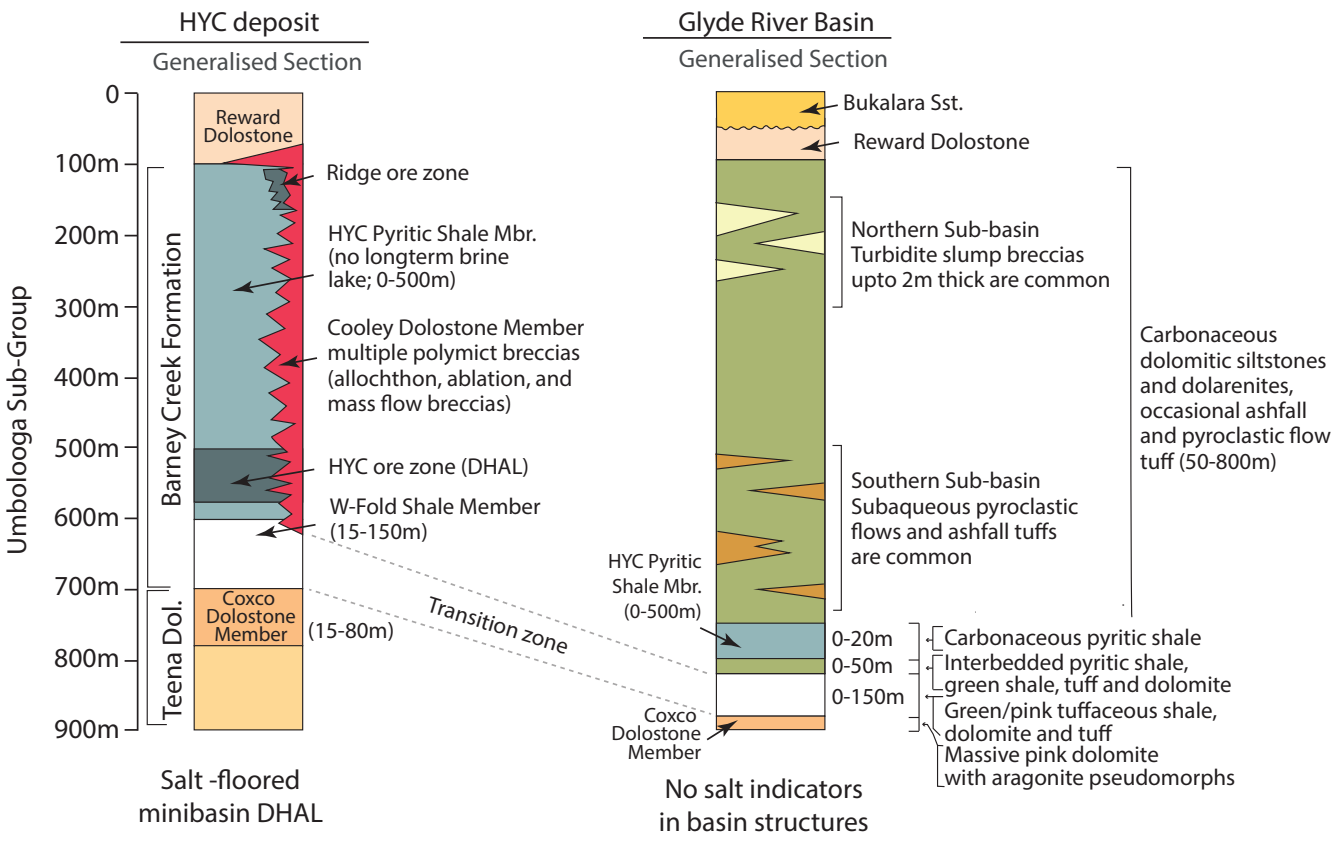

Figure 7. Generalised stratigraphic columns for McArthur basin in the vicinity of HYC deposit and for the Glyde Basin (in part after Davidson and Dashlooty, 1993).

Type II breccia beds occur throughout the HYC Pyritic Shale Member but are most common in the upper half of the Member. Clasts are predominantly grey dololutite which occasionally contain radiating clusters of acicular crystal pseudomorphs ("coxcos") indicative of tropical Proterozoic shelf carbonates. The clasts are similar to lithologies in the Emmerugga and Teena Dolomites and are considered to have been derived from these formations. A characteristic of this breccia type, which differentiates it from Type I and III breccias is the absence of green and red clasts, signifying that clasts in Type II breccias were not derived from the Tooganinie or lower formations, but mostly derived by erosion and collapsed of updip shallow-water cemented shelf carbonate layers. Type II breccias lack the well-developed grading seen in Type I breccias. Isopach maps (Figure 6c) and maximum clast-size plots of individual breccia beds show a close correlation and indicate the type II breccias dominate in the southeast of the HYC subbasin.

Type III breccia beds are confined to the uppermost breccia unit of the HYC Pyritic Shale Member in the HYC sub-basin and are equivalent to the Upper Breccia of Murray (1975). This unit consists exclusively of Type III breccias with the exception of several shale beds near the base. The top of the Upper Breccia is not exposed in the sub-basin, and the unit reaches a maximum known thickness of 210 m. Clasts within the breccias are completely chaotic, and there is no recognisable grading or sorting. Clasts range in size from a few millimetres up to several tens of metres. The fragment lithologies are identical to those in the Type I breccias with the notable exception that they also contain clasts of sandstone, quartzite and potash-metasomatized quartz dolerite—lithologies that are characteristic of the underlying Masterton Formation. The fragments are therefore considered to be derived from the McArthur Group (below the Barney Creek Formation) and the Masterton Formation. According to Walker et al. (1977), the most likely source of the clasts from the Masterton Formation is erosion uplifts and horsts in the Emu Fault Zone. But the same authors also state the exact source area and the direction of movement of the clasts could not be identified. In my opinion, Type III breccias are salt-ablation derived and so contain a variety of clasts lithologies plucked by the rising salt as it rose toward the surface to feed an at-seafloor allochthon.

More broadly, breccias of the updip Cooley Dolostone member, that interfinger and also overlie the HYC deposit (Figure 6a) are usually regarded as part of the Barney Creek Formation. The Cooley Dolostone is interpreted, historically, as a talus slope breccia (Walker et al. 1977, Logan 1979), containing clasts eroded from the Teena and Emmerugga Dolostones. Hinman (1995) regarded the Cooley Dolostone as a tectonic breccia, formed along reverse faults within the steep to overturned, brittle dolomitic lithologies of Teena, Mitchell Yard and Mara Dolostones(members of the Emmerugga Dolostone) as they were overthrust against and over Barney Creek Formation lithologies. Perkins & Bell (1998) interpret the Cooley Dolostone as an in situ alteration body, contiguous with, and derived from, the HYC sequence, rather than being separated from it by a thrust fault. I interpret much of the Cooley as a salt allochthon breccia derived from a salt-cored basin edge fault system, now evolved into a salt weld (Table 2).

Brine haloes and mineralisation

Regional-scale potassic alteration of Tawallah Group dolerites and sediments were documented by Cooke et al. (1998), Davidson (1998, 1999). These authors describe fluids responsible for this alteration as oxidised, low-temperature (100˚C), saline (> 20wt % NaCl equiv), Na-K-Ca-Mg-rich brines, and argue that the high salinities and the presence of hydrocarbons are consistent with brine derivation from nearby evaporitic carbonates during diagenesis.

I suggest that saline fluids feeding these haloes came not from the dissolution of evaporites in adjacent bedded carbonate hosts, but from the decay of former fault-fed thick salt allochthon tongues in positions that now are indicated by salt allochthon breccias. These breccias tie back to what were salt-lubricated fault and salt welds. The presence of salt and diagenetic haloes in these features focused tectonic movement and fluid supply in both initial extensional and subsequent compressional stages. As such, this interpretation supports a salt dissolution origin of the brine origins proposed by both Logan (1979) and Hinman (1995). The difference with their interpretations is that I envisage the brine being derived during salt flow emplacement and dissolution, tied to focused fault conduits in a mobile, suprasalt fault complex, atop or adjacent to the now-dissolved flowing and tiered salt mass. I do not think the nearby platform carbonates (with coxcos and smooth-walled cherts) ever contained significant volumes of primary evaporites.

Worldwide and across deep time, most halokinetic basinwide evaporite associations are typified by an initial extensional and loaded set of diapirs evolving into salt-cored fault welds, with subsequent reactivation of these features in compression (Warren, 2016; Chapter 6). Such a framework typifies long-term salt tectonics with inherently changing structural foci across most Phanerozoic halokinetic salt realms, as in the North Sea, the Persian (Arabian) Gulf and most circum-Atlantic salt basins. It is indicative of continental plate-edge evaporites caught up in the Wilson cycle (Warren, 2010).

Near the HYC deposit, Mn-enrichment, particularly of dolomite and ankerite in the W-fold Shale beneath the ore zone, is considered to be related to exhalation of Mn-bearing brines, associated with rifting and basin deepening, before the onset of zinc-lead mineralisation (Large et al. 1998). This too, is consistent with the salt-focused mineralisation hydrology of diagenetic ferroan and Mn-bearing hydrologies of the modern Red Sea halokinetic deeps (Schmidt et al., 2015) and the Danakhil depression in the Quaternary, when it was a marine-fed saline system (Bonatti et al., 1972).

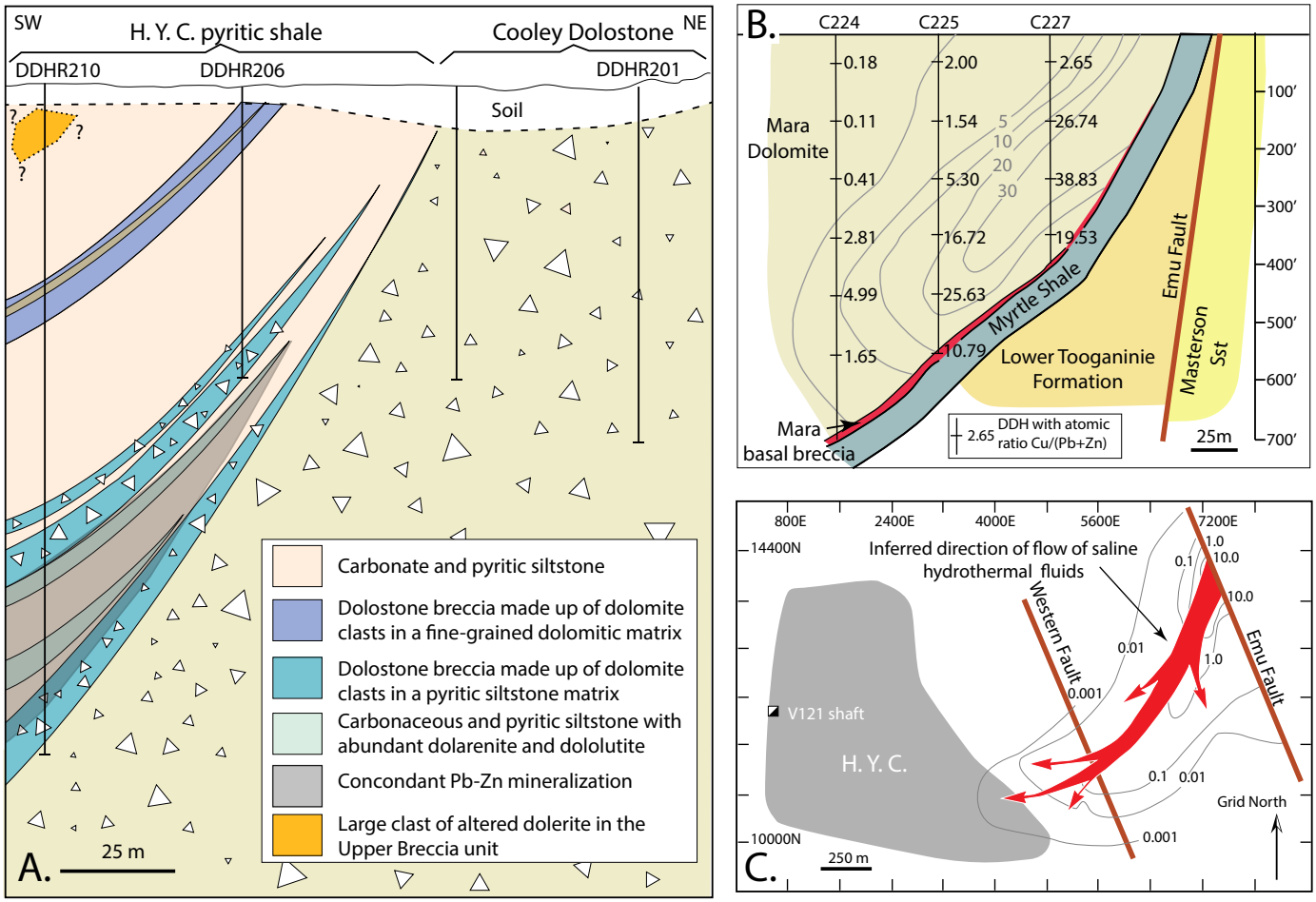

Figure 8. Evolution of Cooley II and Ridge II base metal deposits (after Williams, 1978). A) Cross section through the Ridge II concordant deposit, looking north-west. B) Base metal zoning in a typical section (13,650N) in the Cooley II deposit. C) Direction of flow of mineralizing solutions through the Emmerugga and Cooley Dolostones as inferred from base metal zoning in the discordant deposits.

Ridge and Cooley deposits

In the area to the east of to McArthur River HYC basin, a number of currently sub-economic Zn-Pb-Cu deposits occur, typified by the nearby Ridge and Cooley deposits (Figure 6a; Walker et al. 1977; Williams 1978). Both are similar to the Coxco deposit, being described as MVT deposits mainly hosted by dolomitic breccias, but with minor, shale-hosted concordant mineralisation in the Ridge II deposit (Figure 8; Williams 1978). Likewise, the Coxco deposit contains several million tonnes at 2.5% Zn and 0.5% Pb, in coarse-grained, stratabound galena-sphalerite-pyrite-marcasite, hosted by dolomitic breccias containing clasts of the Mara Dolostone Member, Reward Dolostone, and the Lynott Formation of the McArthur Group, within the Emu Fault Zone (Walker et al. 1977, Walker et al. 1983). Mineralisation comprises veins, "karst" and dissolution breccia fill likened to Mississippi Valley Type (MVT) mineralisation (Walker et al. 1977).

According to Williams (1978), the Emmerugga Dolostone hosts the discordant mineralisation of Cooley II deposit, while Cooley Dolostone breccias contain the Ridge II deposit (Figure 8). The Emmerugga Dolostone at Cooley II consists of massive to laminated dolostone and contains carbonaceous matter, stromatolites, oncolites, and ooids, indicating that it was deposited in a shallow-water normal-marine environment with high biologic productivity. Similarly, the Cooley Dolostone host at Ridge II is a breccia composed of randomly oriented dolostone clasts varying in diameter from a few millimetres up to several tens of metres. Some clasts have near-identical lithologies to those comprising the Emmerugga Dolostone, whereas others contain coxcos and were likely derived from the fragmentation of Teena Dolostone. The Cooley Dolostone breccia contains little depositional matrix. Clast boundaries are marked by sudden changes in features such as dolostone type and bedding-core angles, indicating that the breccia was mostly clast-supported at the time of formation. Most interestingly, drilling in the vicinity of the deposit (DDHR210) intersected a large clast of "out of sequence" dolerite (Figure 8a). Similar large salt-buoyed clasts (up to 100's meters across) composed of Eocene dolerite occur in the salt allochthon breccias at Kuh-e-Namak-Qom (Salty Matters blog, March 10, 2015).

Two major phases of crosscutting brecciation in the area are recognised by Williams (1978) in drill core samples of discordant mineralisation from both the Emmerugga and Cooley Dolostone hosts. First generation breccias, formed during the earlier phase of brecciation, consist of angular clasts of dolostone (< 1 mm to at least 1 m in diameter) in a dark colored matrix of tiny (< 1 μm to 20μm) anhedral dolomite grains, disseminated euhedral pyrite crystals (<50 μm in diameter) and reddish brown carbonaceous matter. The identical nature of the first generation breccias in both the Emmerugga and Cooley Dolostone hosts suggests that brecciation occurred simultaneously in both, via the same mechanism (Williams, 1978). At the time this interpretation was made, there was no "data" (paradigm) available to determine whether the brecciation in the Cooley Dolostone occurred in situ or whether it took place in the dolostone before its removal from the Western Fault Block. Today, we would likely interpret these features as reworked salt ablation breccias on the deep seafloor with infiltrated suspension clays and early-diagenetic pyrite.

Second generation breccias, formed during a later phase of brecciation, consist of angular clasts of first-generation breccias (< 1 mm to at least 10 cm in diameter) in a matrix of either veins filled with sulphide minerals and dolomite, or fine-grained (10 μm to 100 μm in diameter) anhedral dolomite grains, disseminated to massive sulfide minerals, small (on the average 500 μm x 20 μm) interlocking laths of barite or dolomite pseudomorphs after barite, and brown carbonaceous matter (Williams, 1978). Second generation breccias, although coincident with the first generation breccias, are less widespread than the earlier breccias. Again, according to Williams (op. cit.), the similarity of the second generation breccias in both the Emmerugga and Cooley Dolostones suggests a common origin. Again, they concluded there was no "data" (paradigm) available to establish the time of this brecciation relative to the deposition of the Cooley Dolostone. I would argue these "second generation" breccias represent a less distally reworked salt ablation breccia, possibly with interspace anhydrite and gypsum at the time they formed. These calcium sulphate phases facilitated the shallow subsurface emplacement of metal sulphides via bacterial or thermochemical sulphate reduction, in a way not too dissimilar to the mechanisms emplacing Pb-Zn at Cadjebut or Bou Grine ores in Tunisia (Warren and Kempton et al., 1997; Warren 2016; Chapter 15).

Allochthon Interpretation

The origin of the HYC deposit and adjacent subeconomic mineralised accumulations is still somewhat controversial and equivocal (Figure 6a; Ireland et al. 2004a,b; Perkins and Bell, 1998; Logan, 1979; Walker et al., 1977). Large et al. 1998 summarised the alternative models: 1) a sedimentary-exhalative ('sedex') model was proposed by Croxford 1968 and Large et al. 1998; while, 2) a syndiagenetic subsurface replacement model was introduced by Williams 1978; Williams & Logan 1986; Hinman 1995 and Eldridge et al. 1993, the latter based on sulphur isotopes. In my opinion, a third factor, namely a now-dissolved salt allochthon system, should be considered in interpretations of ore genesis and associated breccias. I interpret ore-hosting laminites of HYC deposit as DHAL laminites (Deep seafloor, Hypersaline Anoxic Lake laminites), and the Ridge II and Cooley II were hosted in updip regions once dominated by salt tongues and salt ablation breccias within a fault-fed salt allochthon complex surrounded by updip normal-marine shoal-water platform carbonates (Figure 9).

That is, all three deposits are related to the ongoing and time-transgressive dissolution of shallow halokinetic salt tiers. The salt tongues periodically shed mass flow deposits, triggered by seafloor instability created by the interactions of salt flow, salt withdrawal and the dynamic nature of salt and fault welds. In my opinion, the lack of equivalent breccias, DHAL laminites and halo evidence in otherwise similar deepwater sediment in Barney Creek Formation in the Glyde River Basin, some 80 km to the south-east of HYC, is why this basin lacks economic levels of base metal mineralisation (Figure 7).

Assuming that the first and second generation breccias in Type 1 and III breccias in all of the stratigraphically discordant deposits (allochthon and weld breccia), first defined by Walker et al., 1977 (Table 2) had shared salty origins, the wider distribution of the first generation breccias suggests that they formed via seafloor reworking processes acting across the whole region as a rim to discordant mineralisation (Williams 1978). Therefore, Williams (op cit.) argued geologically reasonable causes of the brecciation in the Cooley Dolostone include; movement on the Western and Emu faults, slumping of debris off the Western Fault Block, and stratal collapse due to the dissolution of evaporite minerals. I would argue for

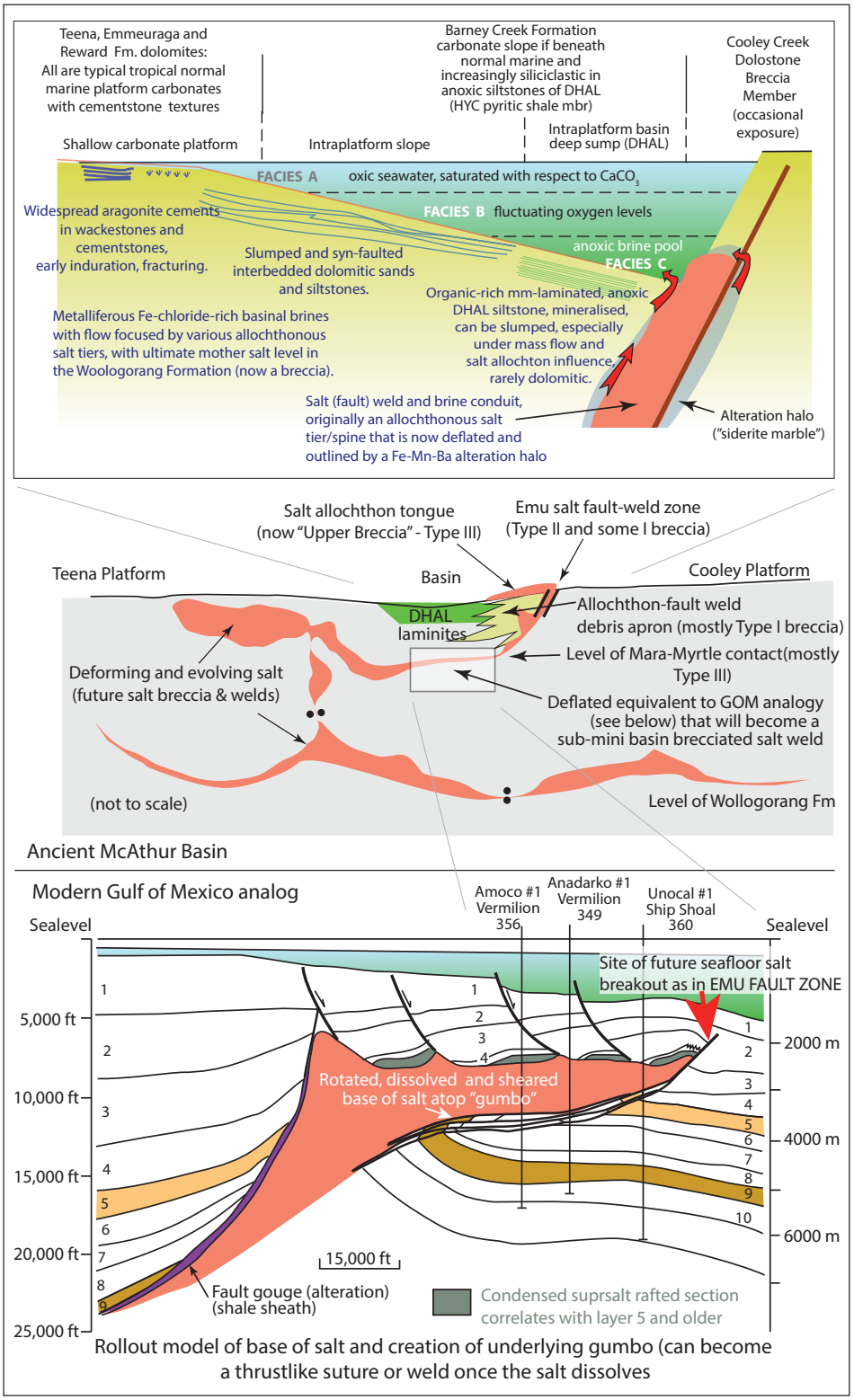

Figure 9. Upper 2 schematic shows an interpreted intra-platform deep setting for mineralised portions of the lower Barney Creek Formation in the vicinity of the HYC, Cooley and Ridge deposits. Seafloor low formed atop salt withdrawal sink adjacent to what is now an inverted basin -edge fault weld (See Warren 2016, Chapter 15, for a detailed description of Facies A, B, C). The lower panel is based on an interpretation of a typical salt allochthon tongue and its stratigraphy, as seen in the modern Gulf of Mexico where Jurassic salt is rolling out across the modern seafloor (after Harrison and Patton 1995).

all of the above, but add that the whole Cooley Dolostone breccia system at the time the first generation breccias formed was a massive salt-flow fault-feeder system that was salt-allochthon cored and salt-lubricated.

Situated at and just below the deep seafloor, salt tongue dissolution created salt-ablation breccias, while the halokinetic-induced seafloor instability instigated periodic mass flows into a metalliferous brine lake; as occurs today in the modern Red Sea deeps, the Orca basin in the Gulf of Mexico and the various brine lakes (DHAL's) of the Mediterranean Ridges (Table 2).

Breccia textures in a halokinetic salt ablation system are always two stage (Warren, 2016); the first stage of brecciation occurs as the salt tongue is inflated and spreading over the surrounds, even as its edges dissolve into ablation breccias reworked by further salt tongue movements and accumulations of contemporary salt-carapace materials (Figure 9). This first stage is typified by mass wasting piles related to the debris rims accumulating about the salt tongue edges, as debris slides downslope across the top of a continuously resupplied salt mass. The friction along the underside of the expanding salt sheets drives overturn, contortion, and brecciation of the underlying deep seafloor bed, this ultimately creates subsalt thrust overfolds (known as gumbo zones beneath the salt allochthons of the Gulf of Mexico). The second stage of brecciation is related to the dissolution of the salt itself once the salt supply is cut off by salt withdrawal and overburden touchdown.

Because allochthons are set up in the expansion stage of salt movement across the seafloor, Stage 1 breccias tend to be more widespread at the landsurface than stage 2 breccias. Stage 2 breccias form once the mother salt supply to the salt tongue or tier is cut off, the salt tongue then dissolves and final brecciation occurs, often with significant roof collapse features in any overburden layers. Similar two-stage allochthon breccias outcrop and subcrop in salt namakier provinces across Iran (Warren 2016, Chapter 7). However, unlike Iran the HYC laminites and associated breccias accumulated in a local deeper marine anoxic sump within a dominant subaqueous normal-marine carbonate shelf setting. There are also partial analogies with salt-cored Jurassic shelf carbonates and allochthon breccias in the paleo Gulf of Mexico, or the Cretaceous mineralised and ferruginised shelf-to-slope halokinetic-cored depositional system that now outcrops in the Domes Region of North Africa (Warren, 2008; Mohr et al. 2007).

Based on the sedimentology of the HYC ore host (Figure 9), I conclude that the HYC deposit accumulated as classic DHAL deposit in a salt allochthon-floored sump. Initial ore accumulation took place as metalliferous laminites in a local salt withdrawal basin. The anoxic brine-filled DHAL sump sat atop a deflating salt allochthon sheet with one of the tiers indicted by salt dissolution breccias at the Myrtle-Mara contact.

The following observations further support this conclusion; 1) the scale and deepwater setting of the deposit, 2) the fault-bound brine-fed margin to the deposit, 3) the rapid local subsidence of the sediments in the deeper water anoxic portion that constitutes the Barney Creek Fm host (HYC Pyrite member), 4) the syndepositional nature of the inter-ore polymict mass flow breccias, 5) the presence of syndepositional barite and Mn haloes from a diagenetically imposed oxidised saline set of pore waters hosted in what were formerly normal-marine sediment pore fluids.

Salt flowing from an allochthon sheet into salt risers in the Emu-Western fault region drove fault-bound rapid subsidence that created local deeper-water anoxic brine-filled sumps in an otherwise healthy marine carbonate shelf (see Salty Matters blog, April 29, 2016, for a salt-controlled structural analogy in the Red Sea). The fault-controlled salt risers allowed brine to escape onto the seafloor at Barney Creek time and to flow across the seafloor into the large DHAL sump that is today the HYC deposit (Figure 9). With time, the salt risers evolved in salt welds and ultimately into fault welds with salt-ablation breccia textures.

The characteristic Fe-Mn and baryte haloes, along with skeletal halites, in what were porous sandstone aquifers intersected by hypersaline waters from the rising and dissolving salt mass are today indicators of the geometry of the former briny plumbing. In the Barney Creek Fm., the occurrence of the Mn and ferruginous haloes indicate the fault-conduit aquifer focus to the suprasalt brine flow and the level of hypersaline brine intersections. There are also transitions into more-typical more-oxidised marine pond and pore water masses in the upper levels atop the DHAL waters and around the edge of its brine curtain.

Williams (1978) concluded the less widespread second generation breccias in the Cooley Dolostone wedge likely formed by processes that acted only locally on the first generation breccias. I agree and would argue that a later DHAL mineralisation focus, during the creation of a later generation of breccias, was the transition from a salt feeder supplying a canopy of allochthon tongues along the Emu Fault region into a system that became first a salt weld, then a fault weld as the mother salt supply was lost (Table 2).

Williams (op. cit.) noted that the association of the two breccia generations, and the occurrence of base metal sulfide minerals and barite, presumably brought in from an outside source, in the matrix of the second generation breccias suggest that the later breccias formed by solution collapse following the introduction of mineralizing solutions into the porous, first generation breccias. I am in complete agreement with this conclusion. In addition, we now have a set of salt-related mechanisms and time-transgressive paradigms that explain the transition from one breccia generation tied to a syndepositional DHAL-related succession that we classify as the sedex brine pool stage that is forming the HYC deposit. With time and salt dissolution/source depletion, we pass to the next generation of breccias, which are linked to a fault weld, evaporite-collapse sub-economic set of MVT deposits (e.g. Cooley II Ridge II and Coxco deposits).

In my opinion, halokinesis created shallow allochthonous salt tiers at the time the normal-marine Emmerugga and Teena Dolostones. Salt withdrawal from allochthon sheets emplaced below the shallow sea floor caused it to deepen locally, this facilitated deposition of thickened intervals of deeper water, more siliceous deposits, as defined by thickness and mineralogical/ colour changes in the W-Fold shale and Barney Creek Formation (Figure 9). Where the brine accumulated in the deepened seafloor depression, which was the HYC DHAL sump, it lay atop a salt withdrawal basin, associated with flow of allochthon salt into the proto-Western Fault (now a deformed fault-weld). The stratigraphic level of the withdrawal is indicated by the allochthon collapse breccia seen at the top of the Myrtle Shale.

The salt-brine focusing time-transgressive halokinetic architecture of the mineral system allowed metal-bearing chloride rich brines circulating in the buried sediments of the basin to access and replace the reduced pyritic and bituminous laminite of the DHAL. As well as ponding in DHALs, some of the same metal-bearing brines exploited the presence of fractionally dissolved interclast calcium sulphate within diapir collapse breccias. So a similar set of redox interfaces drove discordant mineralisation in second generation breccias in the nearby Cooley, Coxco and Ridge deposits. At that time, some of the collapsing crests on the diapiric basin margin perhaps had subaerial crests. We interpret the smaller-scale currently-subeconomic Cooley, Coxco and Ridge deposits as combinations of passive infill, vein and replacement mineralisation in diapiric, dissolution and salt collapse breccias. The Pb-Zn ore, and its collapse-induced host rock, formed in a diagenetic setting much like that in suprasalt circum-diapir MVT deposits hosted in caprocks breccia and peripheral Cretaceous seafloor DHAL laminites in the Bahloul Formation of Northern Africa (see Warren 2016; Chapter 15).

The intimate relationship between breccias and mineralisation across the McArthur River region, including clasts of ore in sedimentary and diagenetic breccias, can be explained, by continual halokinetic salt movement before, during, and after the main episode of laminite Pb-Zn ore formation. This interpretation of both inter-ore “sedimentary” and Cooley Dolostone member breccias across the region reconciles what were seen as previously conflicting primary versus time-transgressive relationships (e.g., Williams 1978; Perkins & Bell 1988).

The characteristic Mn and baryte haloes, along with skeletal halites, in what were porous sandstone aquifers intersected by hypersaline waters from the rising and dissolving salt mass are today indicators of the geometry of the former briny plumbing. In the Barney Creek Fm., the occurrence of the Mn and ferruginous haloes indicate the aquifer and the level on hypersaline brine intersections with the more typical more oxidised marine water mass and pores water at levels atop the brine lake.

Williams (1978) concluded the less widespread second generation breccias in the Cooley Dolostone wedge likely formed by processes that acted only locally on the first generation breccias. I agree, and would argue that the later mineralisation focus, during the creation of the second generation of breccias, was the transition from a salt feeder supplying a canopy of allochthon tongues along the Emu Fault region into a system

that became first a salt weld, then a fault weld as any ongoing mother salt supply was lost. Williams (op. cit.) in a discussion of the Ridge and Cooley deposits noted that the association of the two breccia generations, and the occurrence of base metal sulfide minerals and barite in the matrix of the second generation breccias, presumably brought in via fluids with an outside source. He suggests that later breccias formed by solution collapse following the introduction of mineralising solutions into the porous, first generation breccias. I agree also with this conclusion but would also place it in the typical saline baryte ore association seen in many salt diapir provinces such as the Walton-Magnet Cove region of Nova Scotia, or the Oraparinna Diapir in the Flinders Ranges, South Australia (see Warren 2016, Chapter 7 for detail on theses and other similar baryte deposits).

In addition, we now have a set of salt-related mechanisms and time-transgressive paradigms that explain the transition from one breccia generation tied to a syndepositional DHAL-related succession we classify as the sedex brine pool that is the HYC deposit, to the next generation of breccias that are linked to a fault weld, evaporite-collapse sub-economic set of smaller scale MVT deposits (e.g. Cooley II Ridge II and Coxco deposits).

In my opinion, halokinesis created shallow allochthonous salt tiers at the time the normal-marine Emmerugga and Teena Dolostones were deposited. Salt withdrawal below the shallow sea floor caused it to deepen locally, this facilitated deposition of thickened intervals of deeper water, more siliceous deposits defined by the W-Fold shale and Barney Creek Formation (Figure 9). Where the brine accumulated in the deepened sea-floor that was the HYC DHAL sump it lay atop a salt withdrawal basin, associated with flow of allochthon salt into the proto-Western Fault (now a deformed fault- weld) with the stratigraphic level of the withdrawal indicated by the allochthon collapse breccia at the top of the Myrtle Shale.

The salt-brine focusing time-transgressive halokinetic architecture of the mineral system allowed metal-bearing chloride-rich brines circulating in the basin to access and replace the reduced pyritic and bituminous laminite of the DHAL. As well as ponding in DHALS, some of the same metal-bearing brines exploited diapir collapse breccias and drove discordant mineralisation and second generation breccias in the nearby Cooley, Coxco and Ridge deposits. At that time, some of the collapsing crests on the diapiric basin margin perhaps had subaerial crests. We interpret the smaller-scale currently-subeconomic Cooley, Coxco and Ridge deposits as combinations of passive infill, vein and replacement mineralisation in diapiric, dissolution and collapse breccias. The Pb-Zn ore, and its collapse-induced host rock, formed in a diagenetic setting much like that in suprasalt circum-diapir MVT deposits hosted in caprocks and Cretaceous seafloor laminites of the Bahloul Formation of Northern Africa (see Warren 2016 Chapter 15).

The intimate relationship between breccias and mineralisation across the McArthur River region, including clasts of ore in sedimentary and diagenetic breccias, can be explained, by continual halokinetic salt movement before, during, and after ore formation.

References

Avila-Salinas, W., 1990. Origin of the Copper Ores at Corocoro, Bolivia. In: L. Fontboté, G.C. Amstutz, M. Cardozo, E. Cedillo and J. Frutos (Editors), Stratabound Ore Deposits in the Andes. Special Publication No. 8 of the Society for Geology Applied to Mineral Deposits. Springer Berlin Heidelberg, pp. 659-670.

Bonatti, E., Fisher, D.E., Joensuu, O., Rydell, H.S. and Beyth, M., 1972. Iron-manganese-barium deposit from the north Afar rift (Ethiopia). Economic Geology, 67(6): 717-730.

Bull, S.W., 1998. Sedimentology of the Palaeoproterozoic Barney Creek formation in DDH BMR McArthur 2, southern McArthur basin, northern territory. Australian Journal of Earth Sciences: An International Geoscience Journal of the Geological Society of Australia, 45(1): 21-31.

Cooke, D.R., Bull, S.W., Donovan, S. and Rogers, J.R., 1998. K-metasomatism and base metal depletion in volcanic rocks from the McArthur basin, northern territory - Implications for base metal mineralization. Economic Geology, 93(8): 1237-1263.

Cox, D.P., Lindsey, D.A., Singer, D.A., Moring, B.C. and Diggles, M.F., 2007. Sediment-Hosted Copper Deposits of the World: Deposit Models and Database. USGS Open File Report 03-107, Version 1.3 (Available online at http://pubs.usgs.gov/of/2003/of03-107/.

Davidson, G.J., 1998. Alkali alteration styles and mechanisms, and their implications for a brine factory source of base metals in the rift-related McArthur Group, Australia. Australian Journal of Earth Sciences, 45(1): 33-49.

Davidson, G.J., 1999. Feldspar metasomatism along a Proterozoic rift-basin margin - "Smoke" around a base-metal "fire" (HYC deposit, Australia) or a product of background diagenesis? Geological Society of America Bulletin, 111(5): 663-673.

Davidson, G.J. and Dashlooty, S.A., 1993. The Glyde Sub-basin - A volcaniclastic-bearing pull-apart basin coeval with the McArthur River base-metal deposit, Northern Territory. Australian Journal of Earth Sciences, 40(6): 527-543.

Eldridge, C.S., Williams, N. and Walshe, J.L., 1993. Sulfur isotope variability in sediment-hosted massive sulfide deposits as determined using the ion microprobe SHRIMP: II. A study of the H.Y.C. deposit at McArthur River, Northern Territory, Australia. Economic Geology, 88(1): 1-26.

Entwistle, L.P. and Gouin, L.O., 1955. The chalcocite-ore deposits at Corocoro, Bolivia. Economic Geology, 50(6): 555-570.

Eugster, H.P., 1989. Geochemical environments of sediment-hosted Cu-Pb-Zn deposits. In: R.W. Boyle, A.C. Brown, C.W. Jefferson and E.C. Jowett (Editors), Sediment hosted stratiform copper deposits. Geological Association of Canada, Special Paper, pp. 111-126.

Flint, S., 1986. Sedimentary and diagenetic controls on red-bed ore genesis; the middle Tertiary San Bartolo copper deposit, Antofagasta Province, Chile. Economic Geology, 81(4): 761-778.

Flint, S.S., 1989. Sediment-hosted stratabound copper deposits of the Central Andes. Geological Association of Canada Special Paper, 36: 371-398.

Fusswinkel, T., Wagner, T., Wälle, M., Wenzel, T., Heinrich, C.A. and

Markl, G., 2013. Fluid mixing forms basement-hosted Pb-Zn deposits: Insight from metal and halogen geochemistry of individual fluid inclusions. Geology, 41(6): 679-682.

Groves, D., I. and Bierlein, F., P. , 2007. Geodynamic settings of mineral deposit systems. Journal of the Geological Society, 164: 19-30.

Groves, D.I., Condie, K.C., Goldfarb, R.J., Hronsky, J.M.A. and Vielreicher, R.M., 2005. Secular changes in global tectonic processes and their influence on the temporal distribution of gold-bearing mineral deposits. Economic Geology, 100(2): 203-224.

Harrison, H. and Patton, B., 1995. Translation of salt sheets by basal shear. Proceedings of GCCSEPM Foundation 16th Annual Research Conference, Salt Sediment and Hydrocarbons, Dec 3-6, 1995: 99-107.

Hinman, M., 1995. Base metal mineralisation at McArthur River: structure and kinematics of the HYC-Cooley zone at McArthur River. Australian Geological Survey Organisation, Record,1995/5.

Hitzman, M.W., Selley, D. and Bull, S., 2010. Formation of Sedimentary Rock-Hosted Stratiform Copper Deposits through Earth History. Economic Geology, 105(3): 627-639.

Holman, A.I., Grice, K., Jaraula, C.M.B. and Schimmelmann, A., 2014. Bitumen II from the Paleoproterozoic Here's Your Chance Pb/Zn/Ag deposit: Implications for the analysis of depositional environment and thermal maturity of hydrothermally-altered sediments. Geochimica et Cosmochimica Acta, 139: 98-109.

Ireland, T., Bull, S.W. and Large, R.R., 2004a. Mass flow sedimentology within the HYC Zn-Pb-Ag deposit, Northern Territory, Australia: evidence for syn-sedimentary ore genesis. Mineralium Deposita, 39(2): 143-158.

Ireland, T., Large, R.R., McGoldrick, P. and Blake, M., 2004b. Spatial distribution patterns of sulfur isotopes, nodular carbonate, and ore textures in the McArthur River (HYC) Zn-Pb-Ag deposit, northern territory, Australia. Economic Geology, 99(8): 1687-1709.

Large, R.R., Bull, S.W., Cooke, D.R. and McGoldrick, P.J., 1998. A genetic model for the HYC deposit, Australia: Based on regional sedimentology, geochemistry, and sulfide-sediment relationships. Economic Geology, 93(8): 1345-1368.

Ljunggren, P. and Meyer, H.C., 1964. The copper mineralization in the Corocoro basin, Bolivia. Economic Geology, 59: 110-125.

Logan, G.A., Hinman, M.C., Walter, M.R. and Summons, R.E., 2001. Biogeochemistry of the 1640 Ma McArthur River (HYC) lead–zinc ore and host sediments, Northern Territory, Australia. Geochimica Cosmochimica Acta, 65: 2317-2336.

Logan, R.G., 1979. The Geology and mineralogical zoning of the HYC Ag-Pb-Zn deposit, McArthur River, NT Masters Thesis, Australian National University, Cannberra, Australia.

Logan, R.G., Murray, W.J. and Williams, N., 1990. HYC silver-lead-zinc deposit, McArthur River. In: F.E. Hughes (Editor), Geology of the mineral deposits of Australia and Papua New

Guinea. Monograph Series - Australasian Institute of Mining and Metallurgy, pp. 907-911.

McConachie, B.A. and Dunster, J.N., 1998. Regional stratigraphic correlations and stratiform sediment-hosted base-metal mineralisation in the northern Mt Isa Basin. Australian Journal of Earth Sciences: An International Geoscience Journal of the Geological Society of Australia, 45(1): 83-88.

Meyer, C., 1988. Ore deposits as guides to geologic history of the Earth. In: G.W. Wetherill and et al. (Editors), Annual review of earth and planetary sciences. Vol. 16. Annual Reviews Inc., pp. 147-171.

Mohr, M., Warren, J.K., Kukla, P.A., Urai, J.L. and Irmen, A., 2007. Subsurface seismic record of salt glaciers in an extensional intracontinental setting (Late Triassic of northwestern Germany). Geology, 35(11): 963-966.

Murray, W.J., 1975. McArthur River HYC lead-zinc-silver and related deposits. In: C.L. Knight (Editor), Economic geology of Australia and Papua New Guinea—metals. Australasian Institute of Mining and Metallurgy, Melbourne, pp. 329-338.

Perkins, W.G. and Bell, T.H., 1998. Stratiform replacement lead-zinc deposits: A comparison between Mount Isa, Hilton, and McArthur River. Economic Geology, 93(8): 1090-1212.

Pirajno, F. and Bagas, L., 2008. A review of Australia's Proterozoic mineral systems and genetic models. Precambrian Research, 166(1-4): 54-80.

Rose, A.W., 1976. The effect of cuprous chloride complexes in the origin of red-bed copper and related deposits. Economic Geology, 71(6): 1036-1048.

Ruffell, A.H., Moles, N.R. and Parnell, J., 1998. Characterisation and prediction of sediment-hosted ore deposits using sequence stratigraphy. Ore Geology Reviews, 12(4): 207-223.

Rutland, R.W.R.R., 1966. An unconformity in the Corocoro basin, Bolivia, and its relation to the copper mineralization. Economic Geology, 61: 962-964.

Savrda, C.E., Cook, R.B. and Petrov, A., 2006. Trace Fossil Preservation by Native Copper, Corocoro, Bolivia. Rocks & Minerals, 81(5): 362-363.

Schmidt, M., Al-Farawati, R. and Botz, R., 2015. Geochemical classification of brine-filled Red Sea Deeps. In: N.M.A. Rasul and I.C.F. Stewart (Editors), The Red Sea. Springer, Berlin, pp. 219-233.

Shockey, P.N. and Renfro, A.R., 1974. Copper-silver solution fronts at Paoli, Oklahoma. Economic Geology, 69: 266-268.

Singewald, J.T. and Berry, E.W., 1922. The geology of the Corocoro copper district of Bolivia. Johns Hopkins University studies in geology -- No. 1.. 117 p.

Walker, R.N., Gulson, B. and Smith, J., 1983. The Coxco deposit - a Proterozoic Mississippi Valley-type deposit in the McArthur River district, Northern Territory, Australia. Economic Geology, 78(2): 214 - 249.

Walker, R.N., Logan, R.G. and Binnekamp, J.G., 1977. Recent geological advances concerning the H.Y.C. and associated deposits, McArthur river, N.Y. Journal of the Geological Society of Australia, 24(7-8): 365-380.

Warren, J.K., 2000. Evaporites, brines and base metals: low-temperature ore emplacement controlled by evaporite diagenesis. Australian Journal of Earth Sciences, 47(2): 179-208.

Warren, J.K., 2010. Evaporites through time: Tectonic, climatic and eustatic controls in marine and nonmarine deposits. Earth-Science Reviews, 98(3-4): 217-268.

Warren, J.K., 2016. Evaporites: A compendium (ISBN 978-3-319-13511-3). Springer, Berlin, 1854 pp.

Warren, J.K. and Kempton, R.H., 1997. Evaporite Sedimentology and the Origin of Evaporite-Associated Mississippi Valley-type Sulfides in the Cadjebut Mine Area, Lennard Shelf, Canning Basin, Western Australia. In: I.P. Montanez, J.M. Gregg and K.L. Shelton (Editors), Basinwide diagenetic patterns: Integrated petrologic, geochemical, and hydrologic considerations. SEPM Special Publication, Tulsa OK, pp. 183-205.

Wilkinson, J.J., Stoffell, B., Wilkinson, C.C., Jeffries, T.E. and Appold, M.S., 2009. Anomalously Metal-Rich Fluids Form Hydrothermal Ore Deposits. Science, 323(5915): 764-767.

Williams, N., 1978. Studies of base metal sulphide deposits at McArthur River, Northern Territory, Australia I. The Cooley and Ridge Deposits. Economic Geology, 73(6): 1005 - 1035.

Williams, N. and Logan, R.G., 1986. Geology and evolution of the H.Y.C. stratiform Pb-Zn orebodies, Australia. Stanford Univ.Pub. Geol. Sci., 20: 57-60.

Wu, C., 2008. Bayan Obo Controversy: Carbonatites versus Iron Oxide-Cu-Au-(REE-U). Resource Geology, 58(4): 348-354.

Saltworks Consultants Pty Ltd
ABN 068 889 127
Kingston Park,
5049 South Australia

Email: enquiries@saltworkconsultants.com

Web Page: www.saltworkconsultants.com